AFRL-RD-PS-
TP-2009-1024

PRELIMINARY VHF RADAR AND HIGH-DATA-RATE OPTICAL TURBULENCE PROFILE OBSERVATIONS USING A BALLOON-RING PLATFORM: POST PRINT

Frank D. Eaton et al.

Nastrom Consulting LLC
5407 Sand Bunker ST
Saint Cloud, MN 56304-4632

1 June 2009

Technical Paper

AIR FORCE RESEARCH LABORATORY
Directed Energy Directorate
3550 Aberdeen Ave SE
AIR FORCE MATERIEL COMMAND
KIRTLAND AIR FORCE BASE, NM 87117-5776

REPORT DOCUMENTATION PAGE

Form Approved
OMB No. 0704-0188

1. REPORT DATE *(DD-MM-YYYY)*	2. REPORT TYPE	3. DATES COVERED *(From - To)*
01/06/2009	Technical Paper	May 30, 2008- Jun 1, 2009

4. TITLE AND SUBTITLE

Preliminary VHF radar and high-data-rate optical turbulence profile observations using a balloon-ring platform: Post Print

5a. CONTRACT NUMBER
FA9451-08-M-0239

5b. GRANT NUMBER

5c. PROGRAM ELEMENT NUMBER
Direct Cite

6. AUTHOR(S)

Frank Eaton, Gregory Nastrom, Demos Kyrazis, Don Black, Wiley Black, Alastair Black

5d. PROJECT NUMBER
Direct Cite

5e. TASK NUMBER
Direct Cite

5f. WORK UNIT NUMBER
Direct Cite

7. PERFORMING ORGANIZATION NAME(S) AND ADDRESS(ES)
Nastrom Consulting LLC
5407 Sand Bunker ST
Saint Cloud MN 56304-4632

8. PERFORMING ORGANIZATION REPORT NUMBER

9. SPONSORING / MONITORING AGENCY NAME(S) AND ADDRESS(ES)

Air Force Research Laboratory
3550 Aberdeen Ave SE
Kirtland AFB NM 87117-5776

10. SPONSOR/MONITOR'S ACRONYM(S)
AFRL/RDSA

11. SPONSOR/MONITOR'S REPORT NUMBER(S)
AFRL-RD-PS-TP-2009-1024

12. DISTRIBUTION / AVAILABILITY STATEMENT

Approved for public release

13. SUPPLEMENTARY NOTES
Accepted for publication in the Optics & SPIE Photonics Conference; Atmospheric and Space Optical Systems; San Diego, CA; Aug 2-6, 2009. OP514. 377ABW-2009-0837; July 2, 2009. "Government Purpose Rights"

14. ABSTRACT
A recent measurement campaign at Vandenberg Air Force Base involved taking simultaneous observations with a VHF radar and high-data-rate (1-micron diameter) platinum wires to sense optical turbulence (from temperature fluctuations). The radar observations produce profiles of the refractive index structure parameter, the turbulent kinetic energy, the eddy dissipation rate, the inner scale, the outer scale of turbulence, and wind speed and direction to an altitude of 20 km AGL. The fine wire measurements were taken from the surface with several sensors mounted on a balloon-ring platform sampling in excess of 3 kHz to balloon burst altitudes (typically above 25 km AGL). The main objectives of this effort are to compare the two measurement techniques and to obtain observations that can address several fundamental turbulence issues of the real turbulent atmosphere related to laser beam propagation. To date, modeling and simulation of laser beam propagation through atmospheric turbulence have relied upon a traditional theoretical basis that assumes the existence of homogeneous, isotropic, stationary, and Kolmogorov turbulence. Results presented from the radar observations include the standard deviation of vertical velocity. A comparison of the profiles obtained from the two measurement techniques is shown and discusses. time series of temperature data obtained from a fine wire probe traversing one radar range gate is presented and discussed. Future measurement and analysis efforts are presented.

15. SUBJECT TERMS
Optical Turbulence, Refractive Index Structure Parameter, Inner Scale, Outer Scale, Eddy Dissipation Rate, Meteorological Parameters, Balloon-Ring Platform

16. SECURITY CLASSIFICATION OF:			17. LIMITATION OF ABSTRACT	18. NUMBER OF PAGES	19a. NAME OF RESPONSIBLE PERSON
					Frank Eaton
a. REPORT	b. ABSTRACT	c. THIS PAGE			19b. TELEPHONE NUMBER *(include area code)*
Unclassified	Unclassified	Unclassified	SAR	36	505- 853-1091

Standard Form 298 (Rev. 8-98)
Prescribed by ANSI Std. 239.18

Preliminary VHF radar and high-data-rate optical turbulence profile observations using a balloon-ring platform

Frank D. Eaton[*], Gregory D. Nastrom[+], Demos T. Kyrazis[#], Don G. Black[%], Wiley T. Black[%], and R. Alastair Black[#]

[*]Air Force Research Laboratory, Directed Energy Directorate
Kirtland Air Force Base, NM

[+]Department of Earth and Atmospheric Sciences
St. Cloud State University
St. Cloud, MN

[#]R-Cubed, Inc.
1028 Tramway Ln, NE
Albuquerque, NM

[%]Ridgeline, LLC
63 Otero Road
Los Lunas, NM

ABSTRACT

A recent measurement campaign at Vandenberg Air Force Base involved taking simultaneous observations with a VHF radar and high-data-rate (1-micron diameter) platinum wires to sense optical turbulence (from temperature fluctuations). The radar observations produce profiles of the refractive index structure parameter (C_n^2), the turbulent kinetic energy (σ_t^2), the eddy dissipation rate (ε), the inner scale (l_o), the outer scale (L_o) of turbulence, and wind speed and direction to an altitude of 20 km AGL. The fine wire measurements were taken from the surface with several sensors mounted on a balloon-ring platform sampling in excess of 3 kHz to balloon burst altitudes (typically above 25 km AGL). The main objectives of this effort are to compare the two measurement techniques and to obtain observations that can address several fundamental turbulence issues of the real turbulent atmosphere related to laser beam propagation. To date, modeling and simulation of laser beam propagation through atmospheric turbulence have relied upon a traditional theoretical basis that assumes the existence of homogeneous, isotropic, stationary, and Kolmogorov turbulence. Results presented from the radar observations include C_n^2, σ_t^2, ε, l_0, and the standard deviation of vertical velocity (σ_w). A comparison of the profiles of C_n^2 obtained from the two measurement techniques is shown and discussed. A time series of temperature data obtained from a fine wire probe traversing one radar range gate is presented and discussed. Future measurement and analysis efforts are presented.

Key Words: Optical Turbulence, Refractive Index Structure Parameter, Inner Scale, Outer Scale, Eddy Dissipation Rate, Meteorological Parameters, Balloon-Ring Platform.

Corresponding author address: AFRL/RDSE, 3550 Aberdeen Ave. SE, Kirtland AFB, NM 87117-5776

1. INTRODUCTION

The intensity of turbulence on scales that fall within the inertial subrange is of importance to the laser propagation and imaging communities. With advances in tracking, pointing, and compensation of laser beams over the past several years, new requirements have been established for improving our knowledge of optical turbulence over the propagation paths. This has stimulated the development of new methodologies to sense the refractive index structure parameter (C_n^2) and derived parameters such as the transverse coherence length (r_0), the isoplanatic angle (θ_0), and the Rytov variance (σ_χ^2). Furthermore, preliminary results show that assumptions of "classical theory" (homogeneous, isotropic, stationary, and Kolmogorov turbulence) are often violated. Detailed observations of these turbulent characteristics including inner and outer scale effects coupled with appropriate beam calculations are required to properly assess the impact of a real atmosphere on beam propagation. These results will then be incorporated into various models. The approach using radar and fine wire measurements as described in this paper are required to address these problems.

The use of radar systems has provided great understanding of the physics of atmospheric turbulence and related turbulence issues. A nearly six-year continuous data set observed with a 50-MHz radar at White Sands Missile Range (WSMR) was used to examine slant path optical turbulence conditions (transverse coherence length, isoplanatic angle, and Rytov variance),[1] examine persistent layers of enhanced C_n^2 in the lower stratosphere,[2] estimate the inner and outer scales of turbulence,[3] study gravity waves and turbulence near thunderstorms,[4] investigate the seasonal variation of gravity wave activity at WSMR,[5] and study the coupling of gravity waves and turbulence.[6] Other MST radar studies relevant to this paper include examining the winds and turbulence at WSMR,[7] estimating the eddy dissipation rates,[8] estimating diffusion coefficients,[9] examining the turbulent effects during the passage of a cyclone,[10] examining the onset of the summer monsoon,[11] defining the seasonal variability of turbulence parameters,[12] examining quasi-monochromatic inertia-gravity waves in the lower stratosphere,[13] and examining the relationship between refractivity intensity and synoptic-scale vorticity.[14] A FMCW radar has ultra sensitivity for sensing turbulence in the planetary boundary layer and senses at high resolution (~2-m range and 12 s for obtaining each profile).[15]

Other Air Force Research Laboratory turbulence measurement programs included aircraft and scintillometer observations,[16] combined aircraft and radar observations,[17] turbulence measurements using a kite and tethered blimp platform,[18]and measurements in complex terrain using an ensemble of sensors (scintillometer, differential image motion monitor, sodar, and tower-mounted fine wire sensors).[19] Similar fine wire probe systems were used on the aircraft, kite/tethered blimp experiments, and on the tower. This design was modified for the fine wire systems as described in this paper for use on the balloon-ring platform.

2. THEORETICAL BACKGROUND

Generally beam calculations are performed assuming "classical" turbulent conditions (Kolmogorov, stationary, isotropic, and homogeneous) and a Gaussian beam shape. Most measurements of C_n^2 and derived quantities such as r_o and θ_o also rely on the same "classical" assumptions. Actual measurements to examine if these assumptions are violated are necessary. The measured results then should be used in beam calculations and compared to beam calculations assuming the "classical" conditions. This will allow the determination of the effects of non-Kolmogorov, non-stationary, anisotropic, and non-homogeneous turbulence conditions found in real atmospheres on laser beams. A practical approach involves using the Mutual Coherence Function since this is convenient to vary parameters of interest. For example, different spectra can be used and ultimately results can be easily compared. Three spectra of interest are

1) the Kolmogorov spectrum $\Phi_n(\kappa) = 0.033 C_n^2 \kappa^{-11/3}$ (1)

2) the von Karman spectrum $\Phi_n(\kappa) = 0.033 C_n^2 \dfrac{\exp\left(-\kappa^2/\kappa_m^2\right)}{\left(\kappa^2+\kappa_0^2\right)^{11/6}}$ and (2)

3) the Andrews spectrum $$\Phi_n(\kappa) = 0.033 C_n^2 \frac{\exp\left(-\kappa^2/\kappa_m^2\right)}{\left(\kappa^2+\kappa_0^2\right)^{11/6}} \mathrm{X}\left[1+1.8(\kappa/\kappa_\ell)-2.5(\kappa/\kappa_\ell)^{7/6}\right] \quad (3)$$

where: $\kappa_m = 5.92/\ell_0$ $\kappa_\ell = 3.3/\ell_0$ and $\kappa_0 = 1/L_0$.

As shown above in equation 1, the Kolmogorov spectrum assumes that there are zero inner scales and infinite outer scales of turbulence. The von Karman spectrum (equation 2) accounts for both scales while the Andrews spectrum (equation 3) additionally allows for incorporating the actual shape of the inner scale. Such comparisons are easily done using the Mutual Coherence Function approach.
VanZandt et al.[20] addressed the problem regarding radar observations concerning C_n^2 and ε and they presented the relationship:

$$\varepsilon = \left(\gamma \overline{C}_n^2 \frac{N^2}{F^{1/3}} M^{-2}\right)^{3/2} \quad (4)$$

where γ is a "constant," $\overline{C}_n^2$ is the mean refractive index structure parameter for the radar volume, N is the Brunt Vaisala frequency $\left[N^2 = g(\partial \ln\theta/\partial z)\right]$ where z is the height and θ is the potential temperature, F represents the fraction of the radar volume which is filled by turbulence, and M is the gradient of the generalized potential index. M is given as:

$$M = -77.6\times10^{-6}\frac{P}{T}\left(\frac{\partial \ln\theta}{\partial z}\right)\times\left[1+\frac{15{,}500q}{T}\left(1-\frac{1}{2}\frac{\partial \ln q/\partial z}{\partial \ln\theta/\partial z}\right)\right] \quad (5)$$

where q is the specific humidity, p is pressure in millibars, and T is temperature in degrees Kelvin.

When considering "optical" turbulence, the humidity contribution as shown in equation 5 is not applicable and the term in square brackets tends to unity. Also in the "dry" atmosphere as found in the upper troposphere and stratosphere, the radio and optical refractivity turbulence are identical. When considering the relationship of ε and optical C_n^2 from point measurements such as using fine wire probes, the ambient temperature and gradient of potential temperature must be known as shown in equation 5 after disregarding the humidity effects. C_n^2 is related to the potential energy contained in the turbulence while ε is a measure of the kinetic energy. Therefore, with an atmosphere near adiabatic (constant potential temperature with altitude), C_n^2 will be small but the kinetic energy as described by ε can have a wide range of values.

Another issue is the interpretation of optical measurements taken over long atmospheric paths to derive desired optical turbulent parameters. The C_n^2 and inner scale are known to vary along the path and this effect on estimating parameters such as the integrated turbulent values from scintillometers, pupil plane imagers, and wave front sensors needs to be studied.

3. METHODOLOGY

Turbulence measurements to investigate the stated scientific goals were taken using a 50 MHz radar and fine wire probes mounted on a balloon-ring platform launched near the radar. Salient features of these systems are described in the next section. Temperature data were measured on the balloon-ring platform with fine wire probes at various separations on a boom. A low level fog layer (approximately 200 m thick) existed at the time of launch. Although all probes functioned at the beginning of the flight, only one survived above about 11 km altitude. It is noteworthy that the 1-micron diameter wire probes were able to survive through the fog layer. The data were received by telemetry at the ground at the sampling rate (typically 3.0 kHz). The results of calculations of power spectral densities (PSDs) and structure functions for the observations of each probe display if certain atmospheric conditions produce non-Kolmogorov turbulence. Results using the various horizontal separations and vertical measurements due to the ascent of the sensors show if the atmosphere is truly isotropic for the scales of interest. The temperature structure parameter (C_T^2) values are found from the fine wire temperature measurements and calculated by the spectral method. The low frequency "roll-off" from the –5/3 power law is used to identify the outer scale while the inner scale is evaluated using the radar observations from the relationship $\ell_0 = 7.4\left(\nu^3/\varepsilon\right)^{1/4}$ where ν is the kinematic viscosity of air and ε is the eddy dissipation rate. Spatial frequency is found by invoking Taylor's hypothesis using the local wind speed, defined by the rise rate of the balloon-ring platform. Values of C_n^2 are found by the relationship $C_n^2 = C_T^2\left(79p/T^2 \mathrm{X} 10^{-6}\right)^2$ using temperature (°K) and pressure (mb) appropriate observations from local sensors.

4. INSTRUMENTATION CHARACTERISTICS AND OBSERVING SITE

A thorough rationale for developing the balloon-ring platform system is described in a companion paper in this conference[21] and comparisons of optical propagation statistics from the fine wire measurements to an accepted profile is documented also in this conference.[22] Therefore only a few salient features are described here for the convenience of the reader. Balloon wakes that contaminate measurements taken from sensors behind an ascending balloon have been documented by Tiefenau and Gebbeken[23] and for constant-level balloons.[24] A new platform was designed to examine balloon wake effects using a large "ring" so that sensors mounted facing upwards on the ring will be uncontaminated by the balloon wake. A photograph of the balloon-ring design is shown in Figure 1. The "ring" is an inflatable polyethylene tube with a pressure relief valve. The "ring" is actually 8-sided with a diameter of about 30 feet and trails the balloon using several risers. The balloon wake passes through the center of the "ring" leaving the measurements uncontaminated. This system was used at Holloman AFB and Vandenberg AFB with several tungsten fine wire (1 μm diameter) sensors to measure high-speed turbulent fluctuations. The sensors are mounted on a 3m long boom with positions of 0m, 0.25m, 1.0m, 1.5m, and 3.0m. The associated electronics allow measurements to be taken over a broad range of turbulent conditions. All channels are fed into a controller board that sends the information to a transmitter. The total instrumentation package including sensors, associated electronics, controller board, transmitter, and antenna weighs only a few pounds, allowing the overall system to fall within the same flight regulations as a conventional radiosonde. Data is received by telemetry and a GPS unit on the package aids in possible recovery. Very accurate calibrations are required to obtain data that can be used to calculate spatial differences of turbulence. The complete system is calibrated in a chamber covering the complete range of temperature anticipated.

The 50 MHz radar as shown in Figure 2 is located at Vandenberg AFB. It has fixed coaxial-collinear antennas at right angles. Beams are directed 15^0 from the zenith at 45^0 and 135^0 azimuth, and one is vertical, permitting the three components of the wind vector to be resolved. The antenna is about 150m in diameter and produces a one-way beam width of 2.9^0. Received power, from which C_n^2, wind speed, and spectral width are derived, is observed for 1 min along each beam. Since the three different beams are sampled consecutively, a full profile is obtained every three minutes. Pulse coding applied to the 8-μs transmitted produces 1-μs nominal pulse lengths to give 150-m resolution along each beam axis. In normal operation, 112 range gates are used to sample from 3.22 -20 km in altitude. The transmitted power of 250 kW leads to a power aperture product of 1×10^8 W m^2.

The site at Vandenberg AFB is established and has considerable facilities (including a balloon launch facility) and equipment required for the efforts described here. The site has been recently upgraded as part of the Western Test

Range and has six new boundary layer radars, six sodars, and 30 instrumented towers that will also provide data for this effort in future efforts. Excellent ground receiving stations exist also.

5. RESULTS

Figure 3 shows the C_n^2 hourly profiles from each oblique beam and time-height displays for June 14, 2007 observed by the 50 MHz radar at Vandenberg Air Force Base. The enhanced turbulence at the top of the planetary boundary layer in the region above 4 km AGL is seen and the structure above about 12.5 km is clearly displayed. The following three figures are displayed in the same manner as Figure 3 and all are results derived from the radar measurements. Figure 4 displays the eddy dissipation rate and inner scale calculated by the relationship discussed in the Methodology section. The turbulent kinetic energy and standard deviation of vertical velocity (a proxy indicator of gravity waves) is shown in Figure 5. Both zonal and meridional wind speeds as well as horizontal wind speed and direction are shown in Figure 6.

Figure 7 shows the profile of C_n^2 derived from the C_T^2 values obtained with the fine wire probe. Since examination of the slopes of the PSDs and structure functions showed that very few examples had slopes representative of Kolmogorov turbulence, the units are not specified. In all, 57 segments were used with slopes varying sporadically. Of interest is that an average of these 57 slopes is 1.596, close to 1.667 as expected for Kolmogorov turbulence. It is therefore suggested that the effective sampling of the radar is Kolmogorov since the radar volume is considerably greater than that sampled with the fine wire probe and many slopes are therefore averaged in the radar sensed volume. Also, one minute is observed on each radar beam. Of interest is the propagation effect of a narrow laser beam traversing the variable conditions as opposed to uniform slopes as addressed in a companion paper in this conference.[22]

Figure 8 shows a time series of temperature measurements taken with the fine wire probe through a 150 m height increment to match the range resolution of the 50 MHz radar. This example is typical of other height increments and displays high speed fluctuations on a lower frequency pattern. The total range is only about 0.06 K over this height interval.

The radar-obtained C_n^2 profiles seen in Figure 3 show only modest agreement to the profile derived from the temperature measurements shown in Figure 7. The lower altitude region shows better agreement than the higher region even considering that the radar will sense somewhat higher in the lower region due to the water vapor contribution as displayed in Equations 4 and 5. The PSD of the high speed temperature measurements just above the fog layer (0.449 km) is shown in Figure 9 and the PSD at 19.451 km is displayed in Figure 10. The contrast is seen in the lower wavenumber region where the higher altitude example shows a large decrease in values under the "fit" line-different from the low altitude example. Proper interpretation of these effects is a work in progress.

6. SUMMARY AND CONCLUSIONS

The preliminary results shown here clearly demonstrate that other phenomena besides "classical" turbulence can produce refractivity turbulence in the atmosphere. Single profiles alone as shown here with the fine wire measurements are useful in identifying such conditions but a time-height record as can be obtained with radar observations is needed to show the evolution of the features through the whole life cycle. Radar observations can clearly show layering of turbulence, gravity wave activity, and time varying events such as Kelvin-Helmholtz instabilities. Radar measurements along with in situ measurements such as described here are essential for a full understanding of the problem. The ensemble of observations can then be used to assess the impact on optical propagation.

7. FUTURE PLANNED RESEARCH

This paper presents some preliminary results and new methodology to examine several issues of optical turbulence. One is to evaluate the impact of real atmospheric turbulent conditions on laser beams by considering the non-classical effects of turbulence. High-resolution measurements will be used and incorporated into theoretical beam calculations. The Mutual Coherence Function is one possible approach for many of the calculations, particularly using different

spectra. Other specific objectives are to examine the relationship between mechanical turbulence and optical turbulence (since this is of interest for some modeling approaches), to investigate radar scattering mechanisms including the "filling factor" ("F" in equation 4) problem, to examine the effect of variable C_n^2 and l_o on extracting turbulent parameters over long paths, and to study the turbulent characteristics of the marine boundary layer with associated littoral zone. From simultaneous VHF radar and balloon-ring system observations, the refractive index structure parameter (C_n^2), the eddy dissipation rate (ε), the inner scale (l_o), and the outer scale (L_o) will be evaluated. Special attention will be taken for evaluating turbulence spectra and intermittency within, at the edge, and outside of turbulent layers. The observations will be analyzed to examine if the atmosphere is isotropic for the scales of interest for lasers as well as determining if the turbulence is Kolmogorov under various atmospheric conditions. This effort provides an observation platform that will ultimately lead to the development and validation of conceptual, statistical, physical models.

ACKNOWLEDGMENTS

Special appreciation is extended to Wayne Stitch and Donald Erikson for their help in planning and coordinating the observation periods at Vandenberg Air Force Base.

REFERENCES

1. F. D. Eaton, G. D. Nastrom, and A. R. Hansen, "Middle atmosphere slant-path optical turbulence conditions derived from VHF radar observations," *Optical Engineering,* **38**, No. 2, 200-207, 1999.

2. G. D. Nastrom and F. D. Eaton, "Persistent layers of enhanced C_n^2 in the lower stratosphere from VHF radar observations," *Radio Science,* **36**, No. 1, 137-139, 2001.

3. F. D. Eaton and G. D. Nastrom, "Preliminary estimates of the inner and outer scales from White Sands Missile Range, NM radar observations," *Radio Science*, **33**, No. 4, 895-903, 1998.

4. A. R. Hansen, G. D. Nastrom, J. A. Otkin, and F. D. Eaton, "MST radar observation of gravity waves and turbulence near thunderstorms," *Journal of Applied Meteorology,* **41**, pp. 298-305, 2002.

5. A. R. Hansen, G. D. Nastrom, and F. D. Eaton, "Seasonal variation of gravity wave activity at 5-20 km observed with the VHF radar at White Sands Missile Range," New Mexico, *Journal of Geophysical Research,* **106**, No D15, 17,171-17,183, 2001.

6. G. D. Nastrom and F. D. Eaton, "The coupling of gravity waves and turbulence at White Sands, New Mexico, from VHF radar observations," *Journal of Applied Meteorology,* **32**, No. 1, 81-87, 1993.

7. G. D. Nastrom and F. D. Eaton, "Variations of winds and turbulence seen by the 50-MHz radar at White Sands Missile Range, New Mexico," *Journal of Applied Meteorology,* **34**, No. 10, 2135-2138, 1995.

8. G. D. Nastrom and F. D. Eaton, "Turbulence eddy dissipation rates from radar observations at 5-20 km at White Sands Missile Range, NM," *Journal of Geophysical Research,* **102**, No. D16, 19,495-19,505, 1997.

9. G. D. Nastrom and F. D. Eaton, "A brief climatology of eddy diffusivities over White Sands Missile Range, New Mexico," *Journal of Geophysical Research-Atmospheres,* **102**, No. D25, 29,819-29,828, 1997.

10. G. D. Nastrom and F. D. Eaton, "A case study of atmospheric conditions at 4-19 km over Vandenberg AFB during passage of a cyclone," *Journal of Applied Meteorology,* **42**, No. 4, pp. 467-475, 2003.

11. G. D. Nastrom and F. D. Eaton, "The onset of the summer monsoon over White Sands Missile Range, New Mexico, as seen by VHF radar," *Journal of Geophysical Research-Atmospheres,* **97**, No. D12, pp. 22,235-22,243, 1993.

12. G. D. Nastrom and F. D. Eaton, "Seasonal variability of turbulence parameters at 2 to 21 km from MST radar measurements at Vandenberg Air Force Base, California," *Journal of Geophysical Research,* **110**, D19110, doi:10.1029/2005JD005782, 2005.

13. G. D. Nastrom, and F. D. Eaton, "Quasi-monochromatic inertia-gravity waves in the lower stratosphere from MST radar observations," (In Press) *Journal of Geophysical Research,* Vol III, doi:10:1029/2006.

14. G. D. Nastrom and F. D. Eaton, "The relationship between refractivity intensity from MST radar observations and synoptic-scaled vorticity," Submitted to *Radio Science.*

15. F. D. Eaton, S. A. McLaughlin, and J. R. Hines, "A new frequency-modulated continuous wave radar for studying planetary boundary morphology," *Radio Science,* Vol 30, No. 1, pp. 75-88, 1995.

16. I. L. Hahn, B. P. Venet, F. D. Eaton, R. J. Hugo, and S. R. Nowlin, "Refractive index structure parameter in the boundary layer as measured from an aircraft and a ground based scintillometer," *American Meteorological Society Paper 3B.2,* 13th Symposium on Boundary Layers and Turbulence, 79th Annual Meeting, Dallas, Texas, 1999.

17. F. D. Eaton, G. D. Nastrom, B. Masson, I. L. Hahn, K. A. McCrae, S. R. Nowlin, and T. Berkopec, "Radar and aircraft observations of a layer of strong refractivity turbulence," Proceedings of the SPIE, **3381,** AeroSense Airborne Laser Advance Technology, Orlando, FL, 1998.

18. F. D. Eaton, B. B. Balsley, R. D. Frehlich, R. J. Hugo, M. Jensen, and K. A. McCrae, "Turbulence observations over a desert basin using a kite/tethered-blimp platform," *Optical Engineering,* **39**, pp. 2517-2526, 2000.

19. F. D. Eaton, W. P. Brown, S. D. Ford, J. E. Miller, S. D. Stokes, and V. M. Stone, "Intercomparisons of turbulence observations in a mountain-valley system," Proceedings of the SPIE, **4376**, Laser Weapons Technology II, 134-140, Orlando, FL, 2001.

20. T. E. VanZandt, J. L. Green, K. S. Gage, and W. L. Clark, "Vertical profiles of refractivity turbulence structure constant: Comparisons of observations by the Sunset radar with a new theoretical model," *Radio Science,* **13**, 819-829, 1978.

21. D. T. Kyrazis, F. D. Eaton, D. Black, W. Black, and R. A. Black, "The balloon ring: a high performance, low cost instrumentation platform for measuring atmospheric turbulence profiles," SPIE Optical Engineering & Applications 2009, Atmospheric Optics, Measurements, and Target-in-the-Loop Propagation III, (this conference), San Diego, CA, 2009.

22. T. Clark, D. T. Kyrazis, and F. D. Eaton, "Comparison of some optical propagation statistics implied by recent atmospheric measurements to those on CLEAR I," SPIE Optical Engineering & Applications 2009, Atmospheric Optics, Measurements, and Target-in-the-Loop Propagation III, (this conference), San Diego, CA, 2008.

23. H. E. Tiefenau, and A. Gebbeken, "Influence of meteorological balloons on temperature measurements with radiosondes: nighttime cooling and daytime heating," *Journal of Atmospheric and Oceanic Technology,* **6**, pp. 36-42, 1989.

24. R. D. Reynolds, and R. L. Lamberth, "Ambient temperature measurements from radiosondes flown on constant-level balloons," *Journal of Applied Meteorology,* **5**, pp. 304-307, 1966.

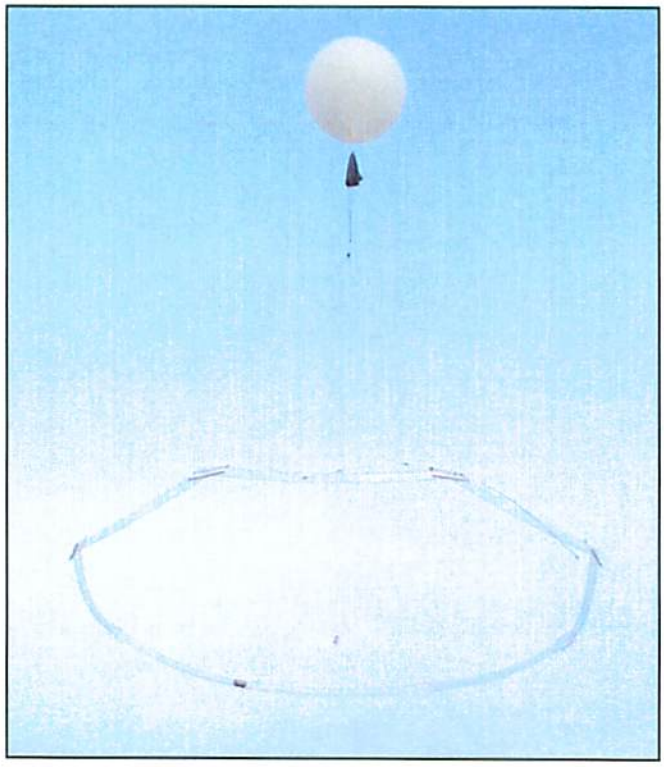

Figure 1. Photograph showing the balloon-ring platform in flight. A parachute is just below the balloon.

Figure 2. Photograph showing the phased array antenna of the 50 MHz radar at Vandenberg Air Force Base. The antenna is 150 m in diameter and the power aperture product is 1×10^8 Wm^2.

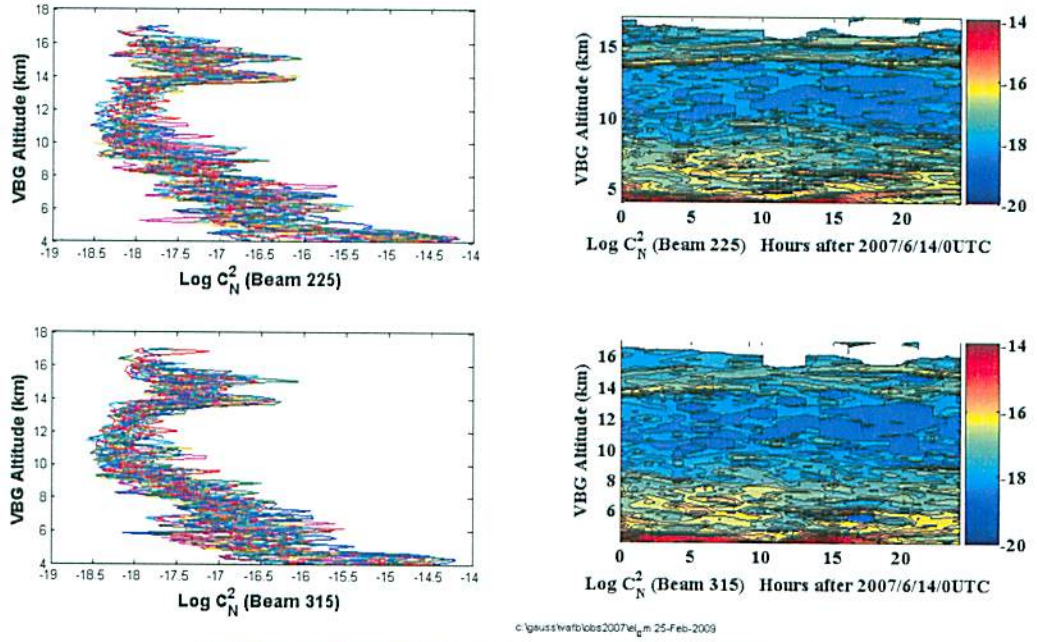

Figure 3: Refractivity turbulence measured by the 50 MHz radar.

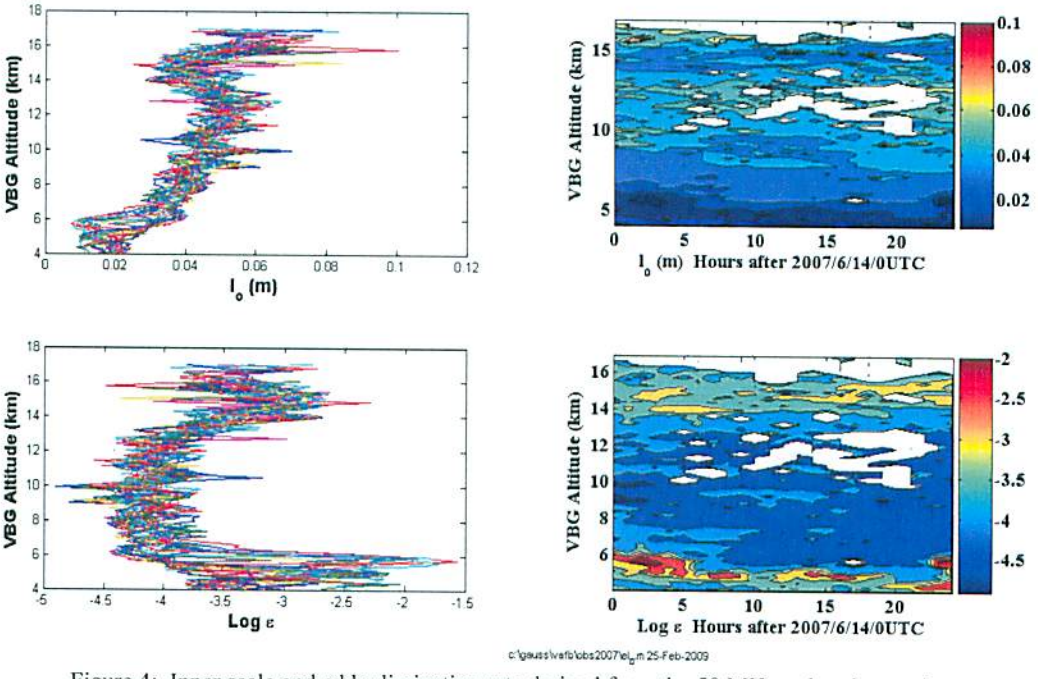

Figure 4: Inner scale and eddy dissipation rate derived from the 50 MHz radar observations.

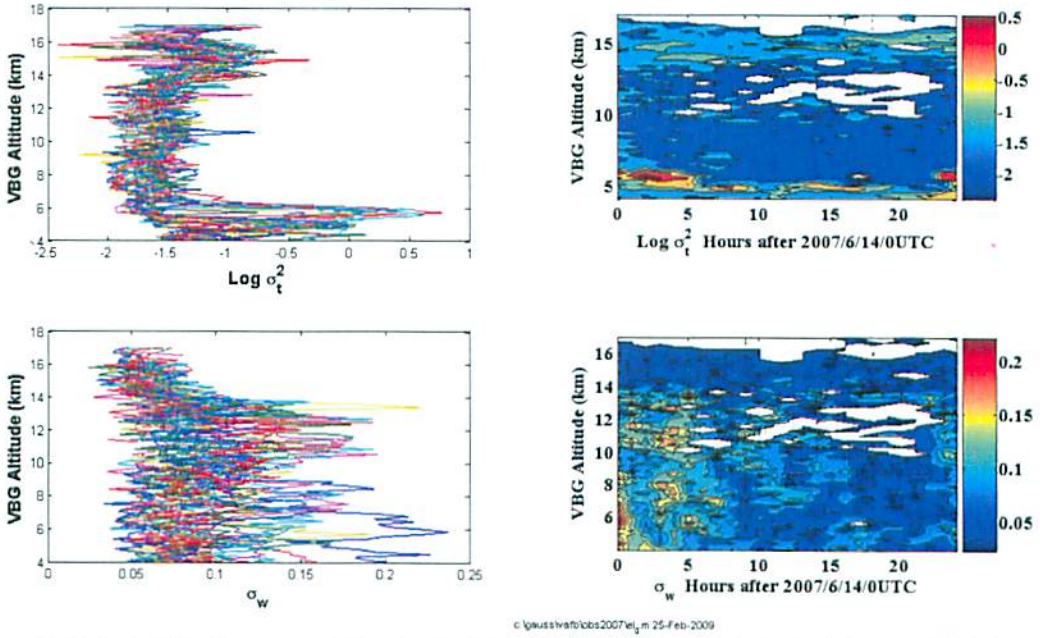

Figure 5: Turbulent kinetic energy and the standard deviation of vertical velocity derived from the 50 MHz radar.

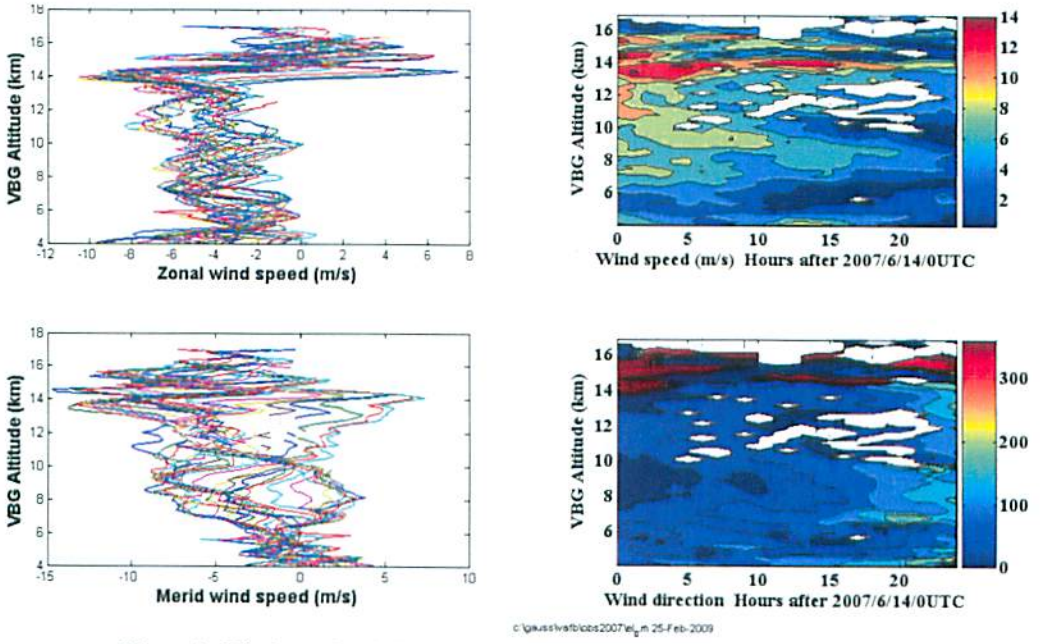

Figure 6: Wind speed and direction derived from the 50 MHz radar observations.

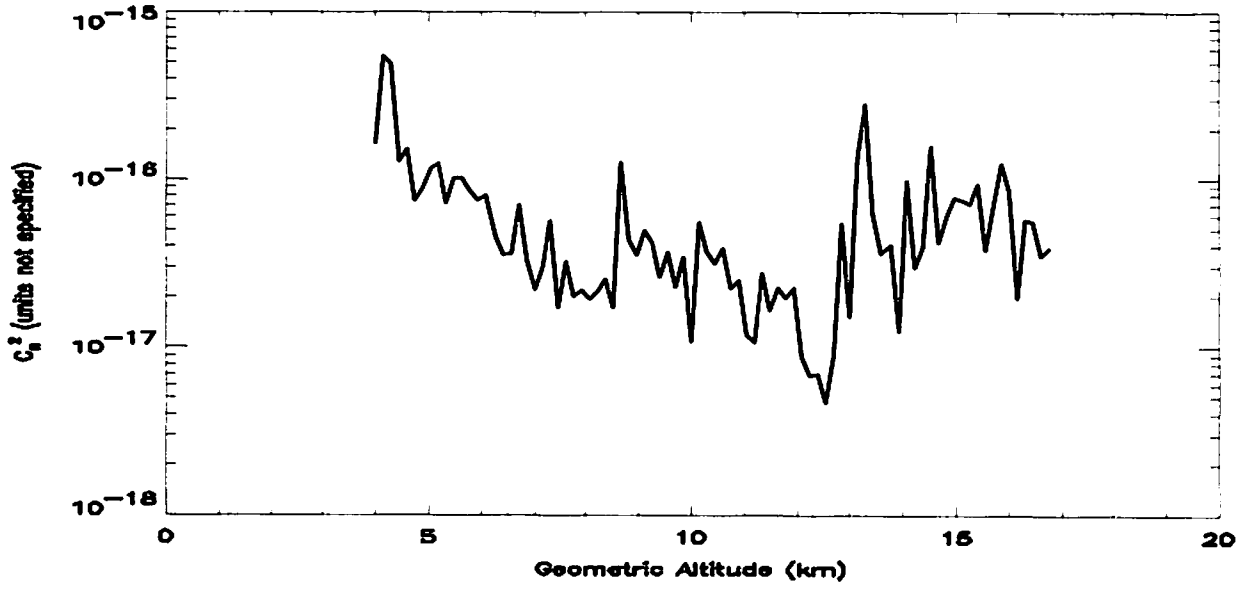

Figure 7: Profile of refractivity turbulence derived from the fine wire probe temperature measurements.

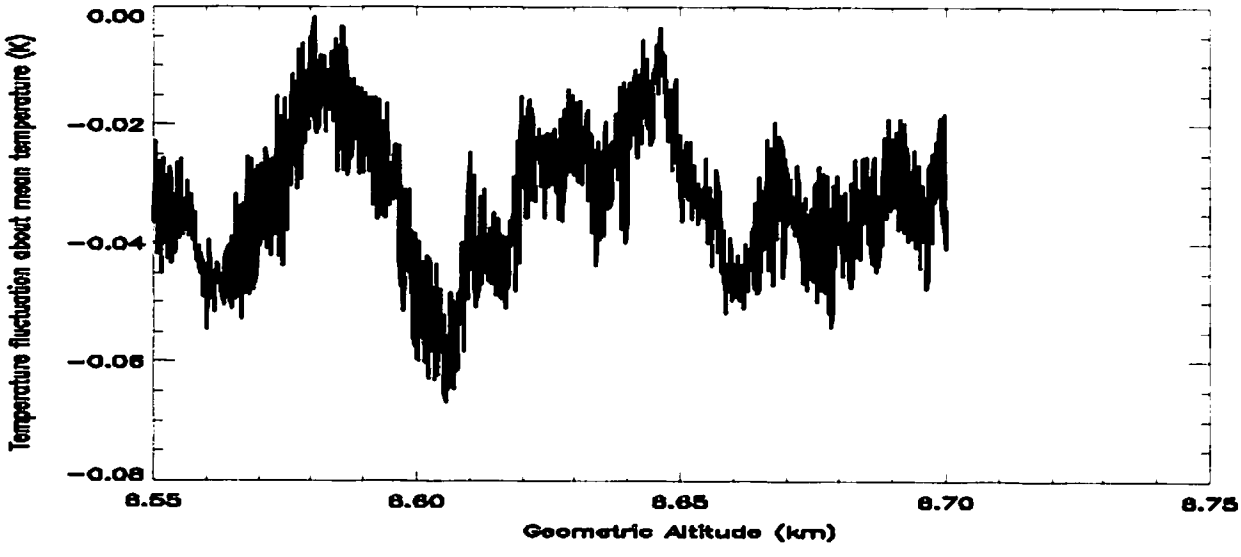

Figure 8: Time series of temperature measurements with the fine wire probe through one range gate (150m) of the radar.

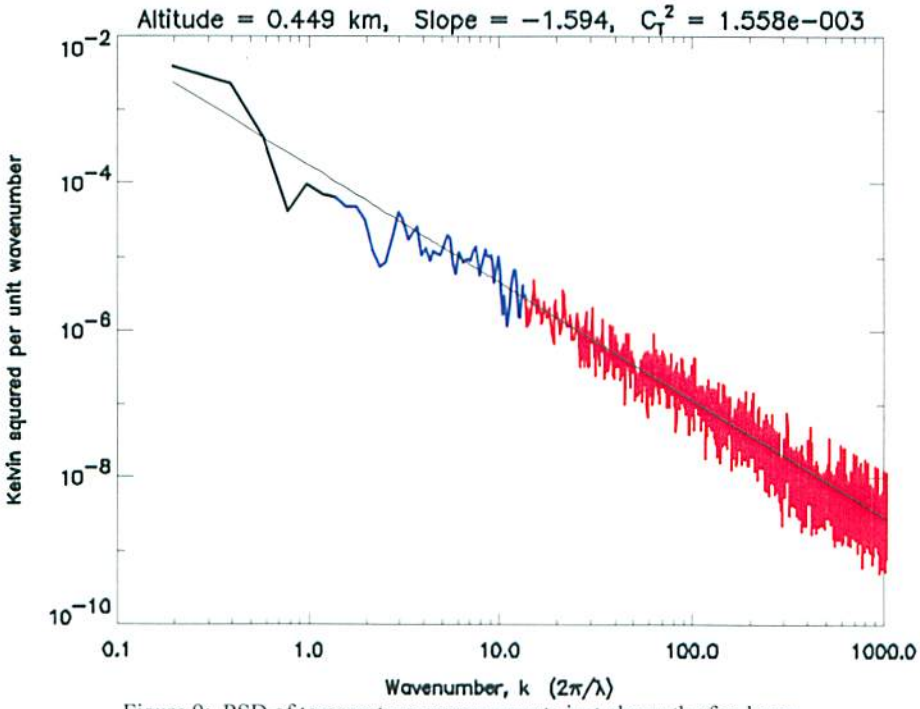

Figure 9: PSD of temperature measurements just above the fog layer.

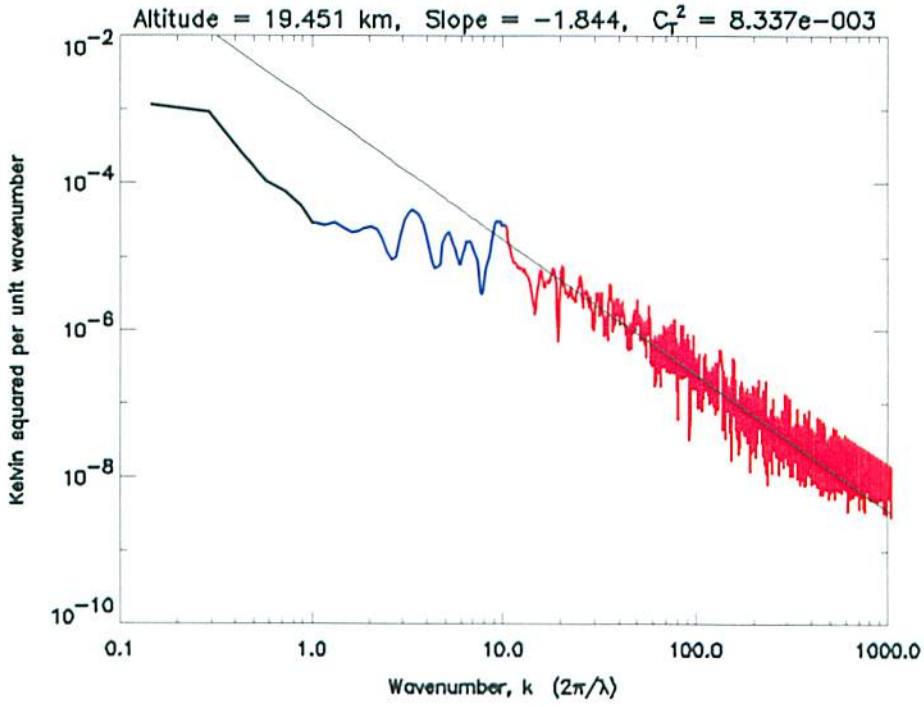

Figure 10: PSD of temperature measurements above 19 km altitude.

Preliminary VHF radar and high-data-rate optical turbulence profile observations using a balloon-ring platform

Frank D. Eaton[a], Gregory D. Nastrom[b], Demos T. Kyrazis[c], Don G. Black[d], Wiley T. Black[d], R. Alastair Black[c]

[a]Air Force Research Laboratory
Kirtland AFB, NM

[b]St. Cloud State University
St. Cloud, MN

[c]R-Cubed, Inc.
Albuquerque, NM

[d]Ridgeline, LLC
Los Lunas, NM

Outline

Issues discussed:

1) The effects of real turbulent conditions on laser beam propagation need to be assessed. These include the non "classical" effects due to non-Kolmogorov, anisotropic, non-stationary, and non-homogeneous turbulence.

2) Various measurement systems need to be compared and validated. This includes in-situ fine wire sensor measurements and Doppler radar observations.

3) The "volume filling" radar problem needs to be addressed.

4) The relationship of mechanical and optical turbulence needs to be examined.

Vandenberg Radar Site

Radar Obtained Parameters

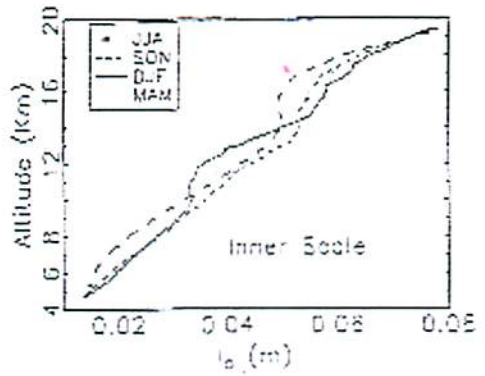

Figure 3. Seasonal vertical profiles of the inner scale of atmospheric turbulence derived from VHF radar measurements over a 5-year period.

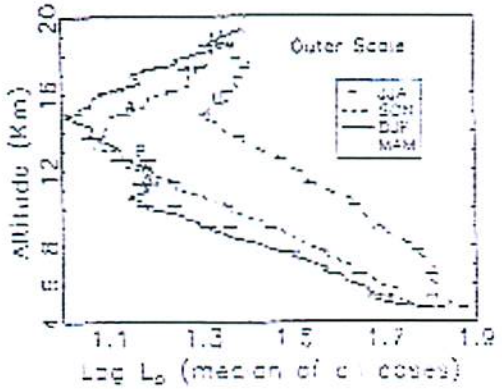

Figure 4. Seasonal profiles of the outer scale of atmospheric turbulence derived from VHF radar measurements over a 5-year period. The error bars plotted relative to each seasonal curve extend ±1 standard error of the mean. Also included are symbols showing average seasonal tropopause heights.

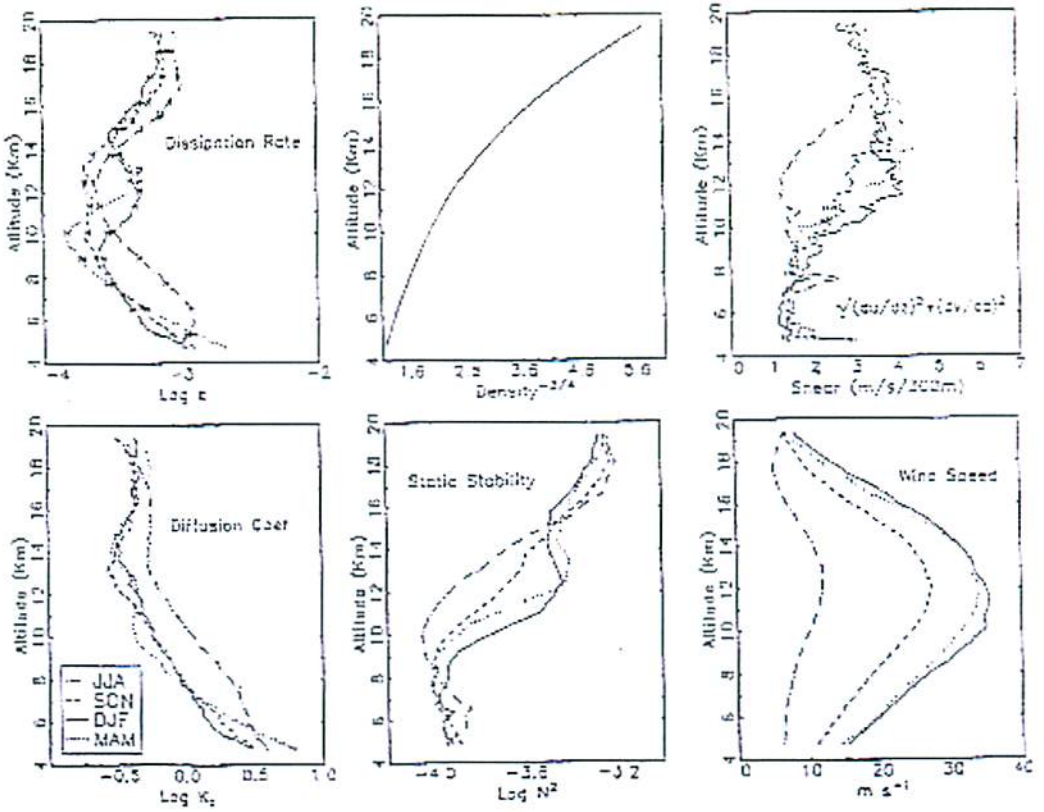

Frank D. Eaton and Gregory D. Nastrom, 1998: **Preliminary estimates of the vertical profiles of inner and outer scales from White Sands Missile Range, New Mexico, VHF radar observations,** *Radio Science,* Vol. 33, No. 4, pp. 895-903.

Temperature, Density, Pressure, and Brunt Vaisala Profiles for June 14, 2007 at Vandenberg Air Force Base

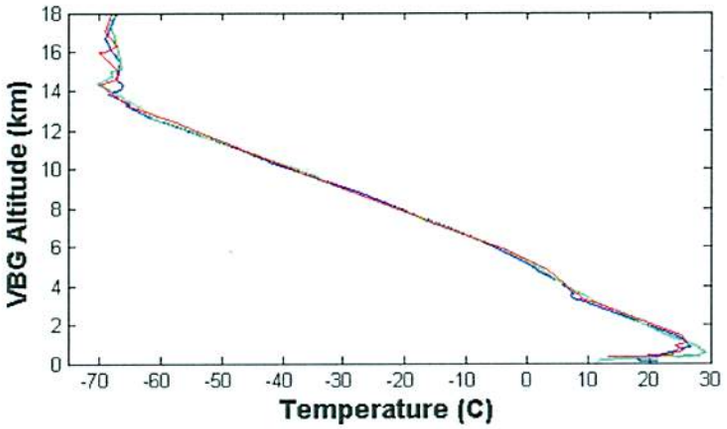

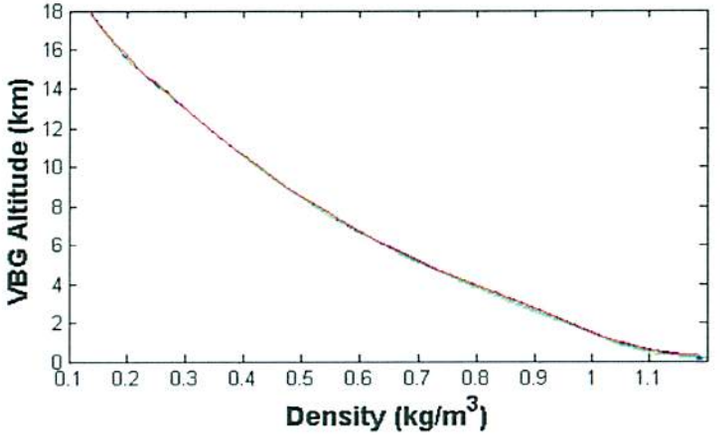

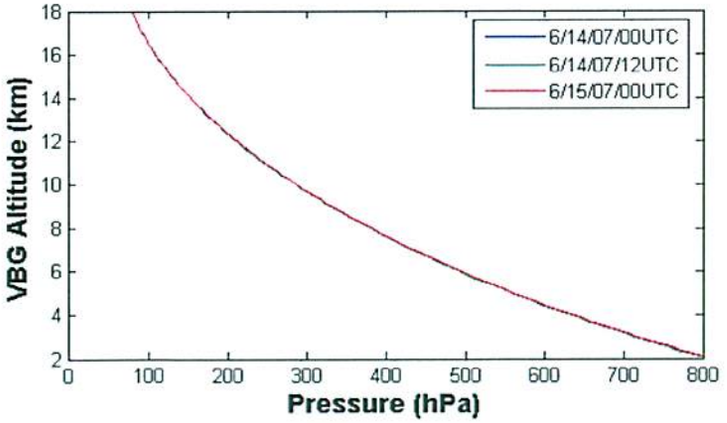

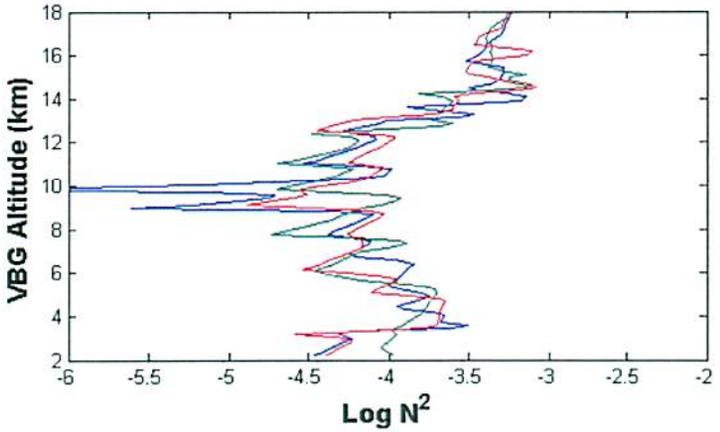

c:\gauss\vafb\obs2007\addraobs.m 25-Feb-2009

Inner Scale and Eddy Dissipation Profiles for June 14, 2007 at Vandenberg AFB

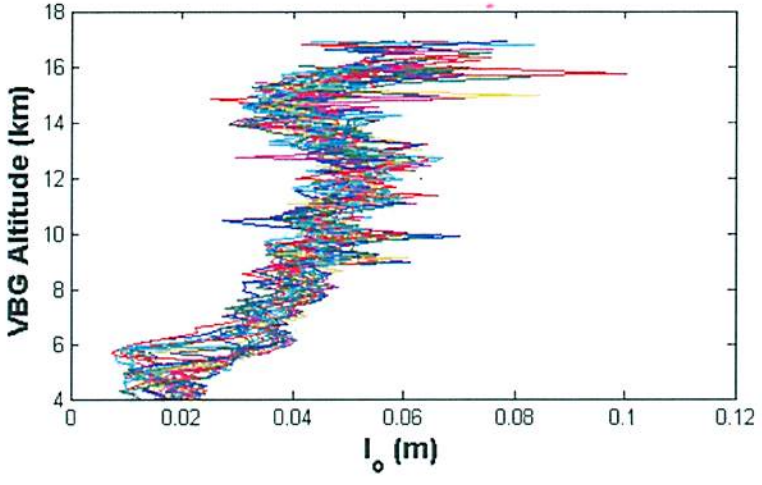

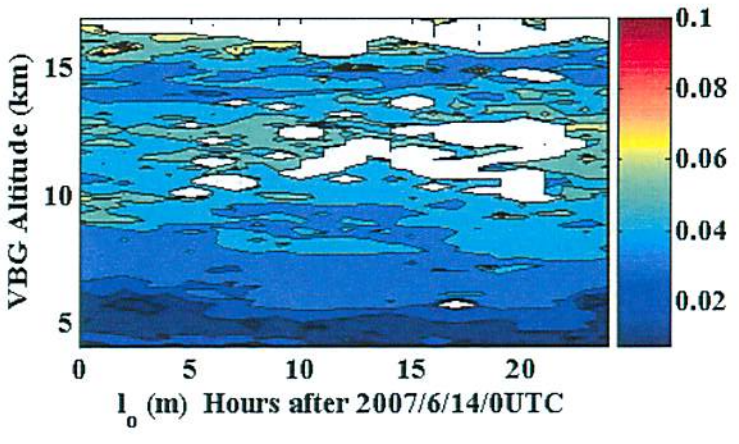

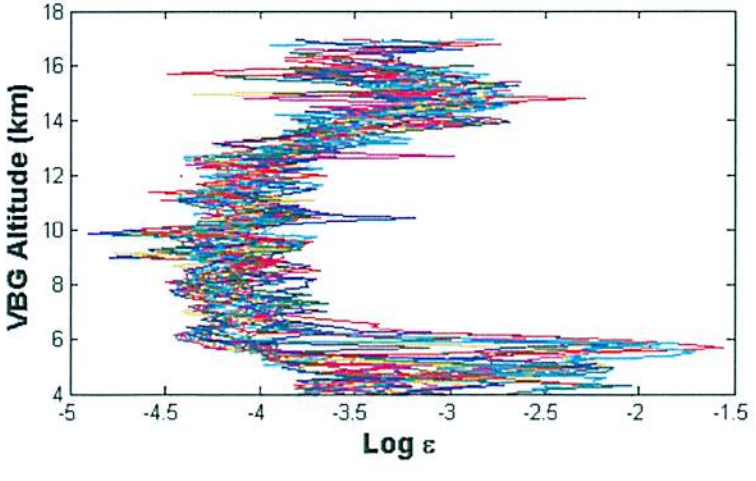

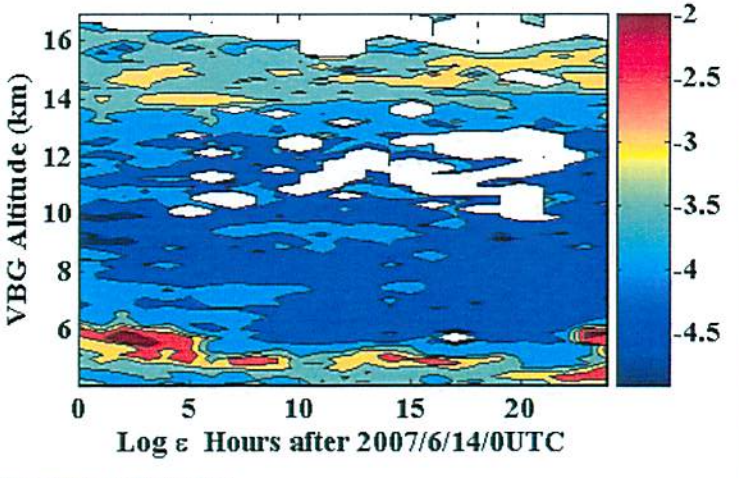

c:\gauss\vafb\obs2007\el$_0$m 25-Feb-2009

Turbulent Kinetic Energy and Standard Deviation of Vertical Velocity for June 14, 2007 at Vandenberg AFB

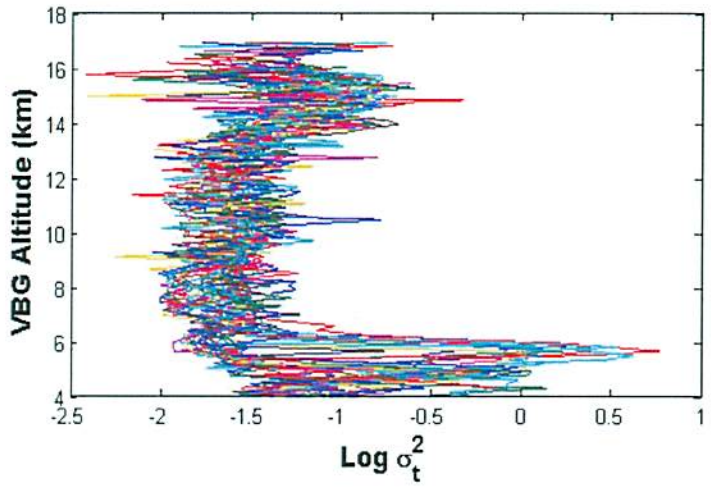

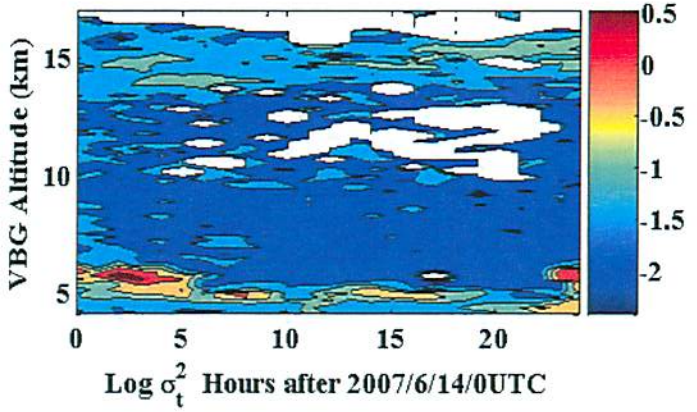

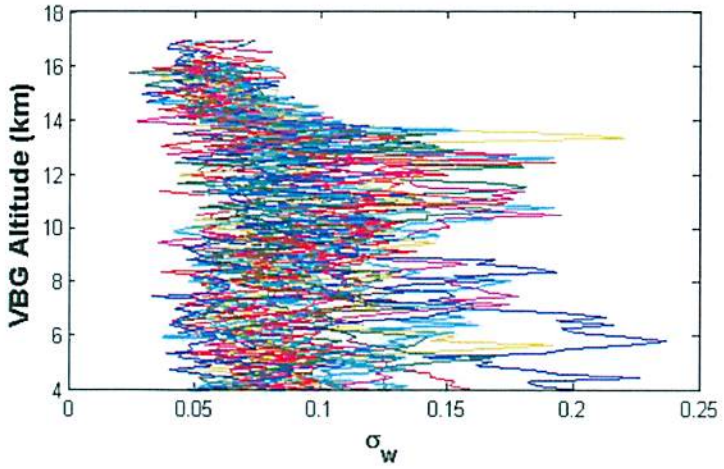

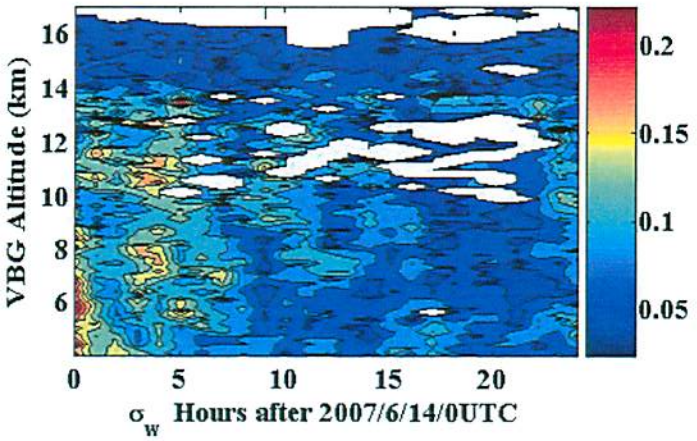

c:\gauss\vafb\obs2007\el_m 25-Feb-2009

Wind Speed and Direction for June 14, 2007 at Vandenberg, AFB

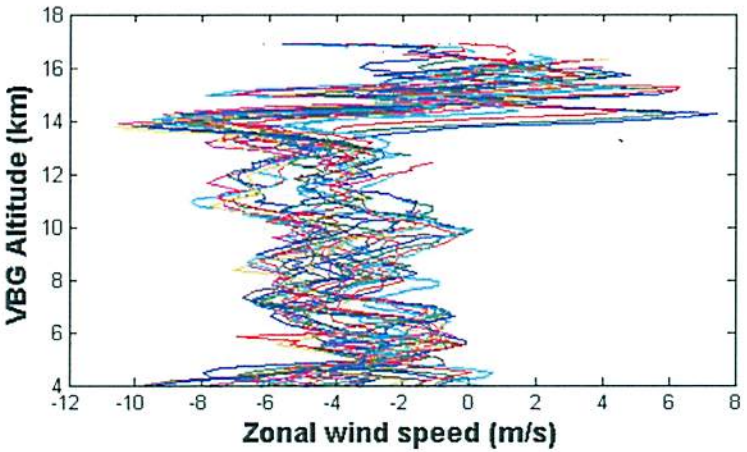

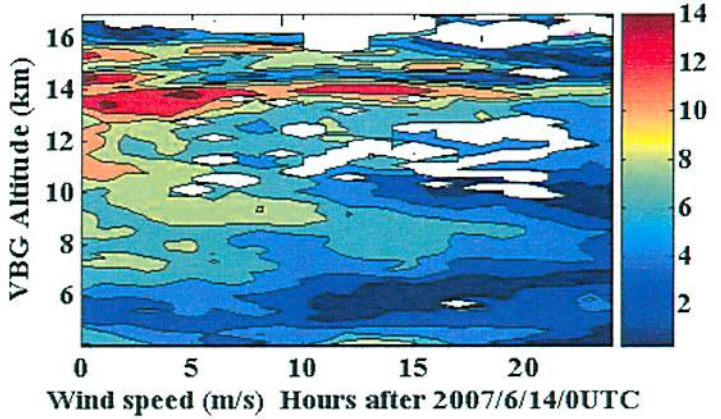

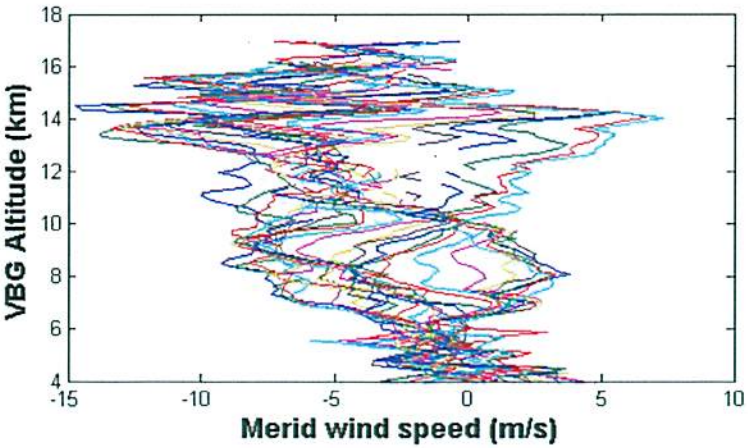

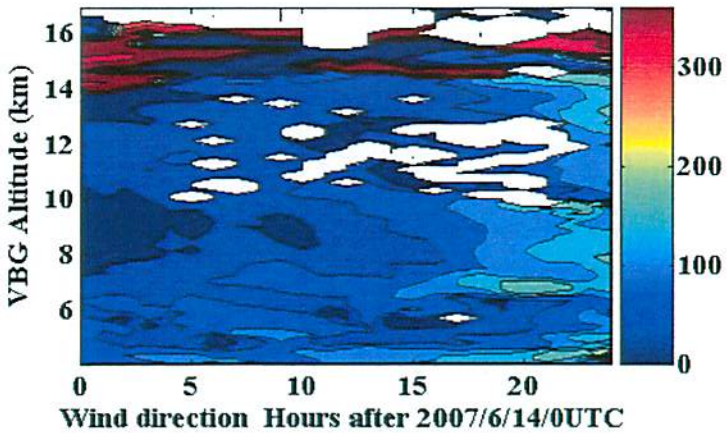

c:\gauss\vafb\obs2007\el_0 m 25-Feb-2009

Refractivity Turbulence for June 14, 2007 at Vandenberg AFB

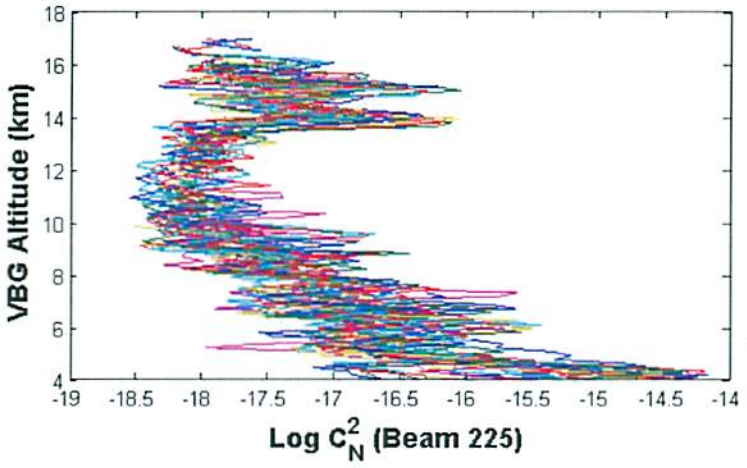

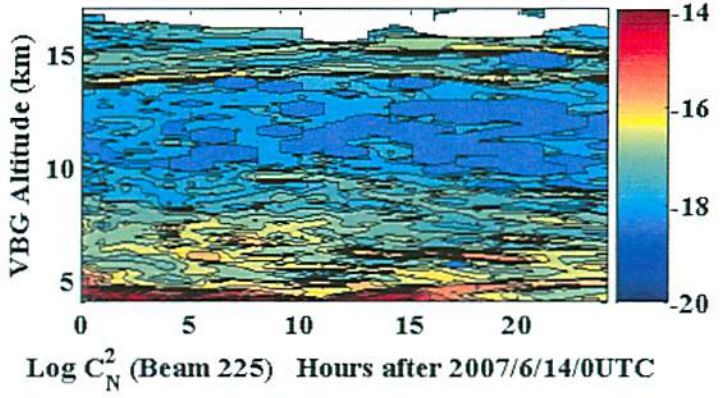

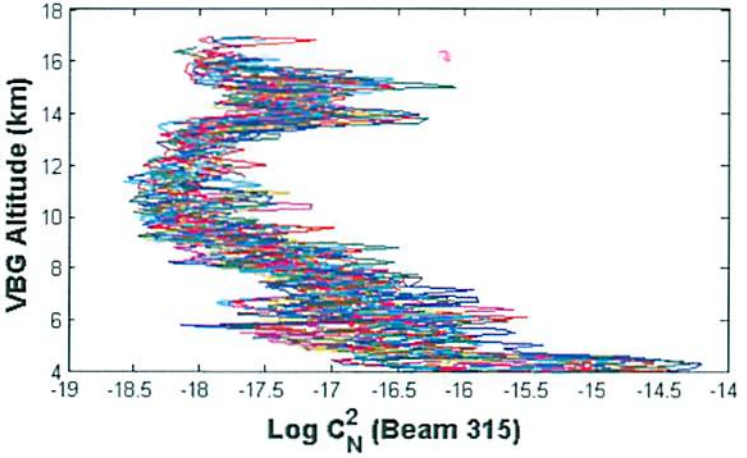

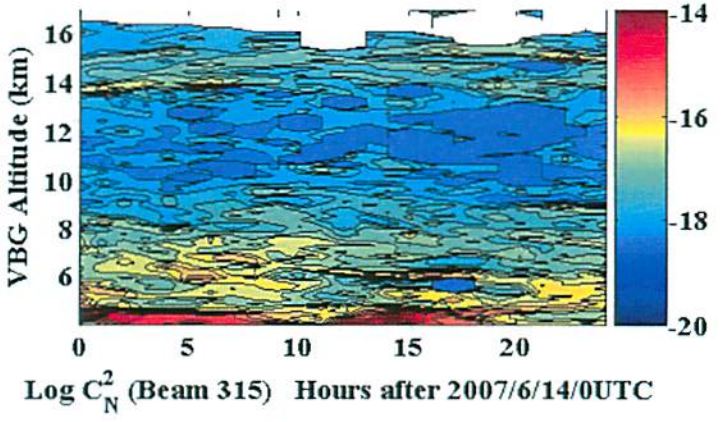

c:\gauss\vafb\obs2007\el$_0$.m 25-Feb-2009

AFRL: Full Flight Envelope

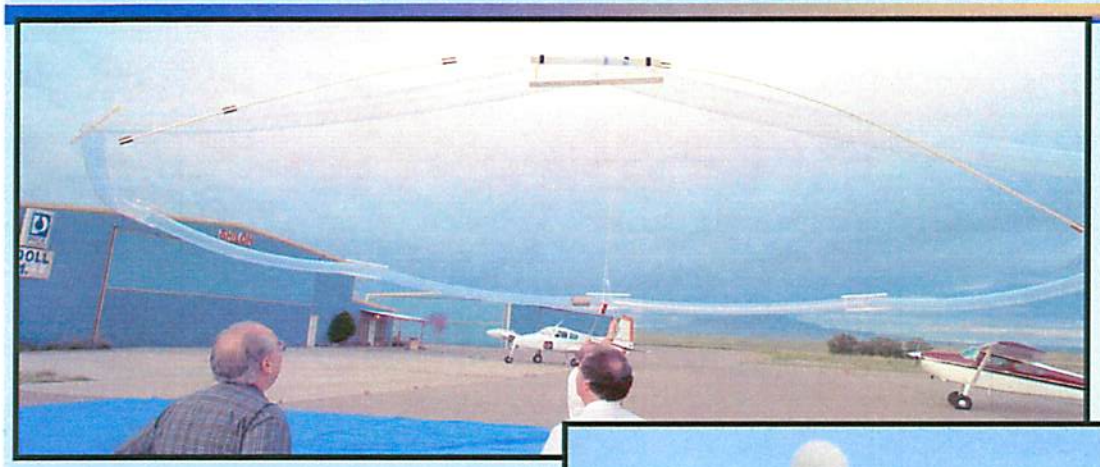

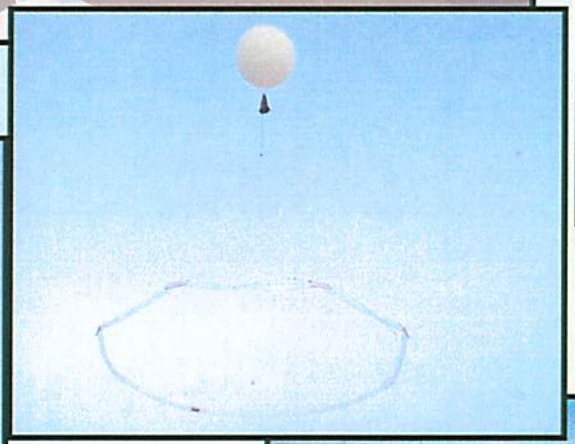

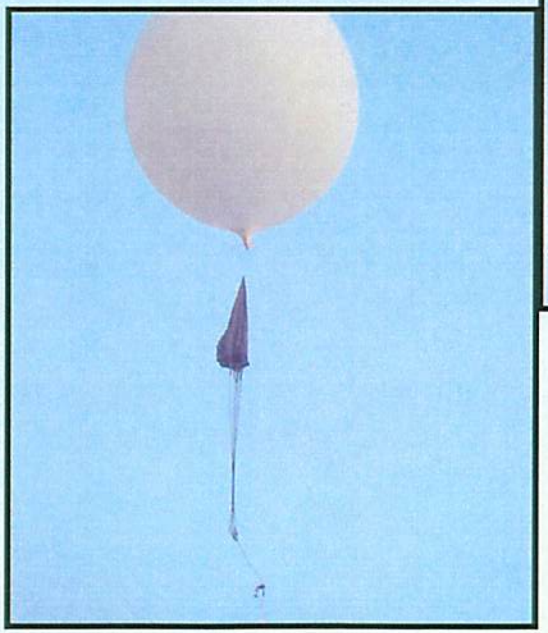

System stability check

-launch forces

-Balloon inflation pressure

-parachute deployment

-Pressure sensitive cut-down

Refractivity Turbulence Profile for June 14, 2007 From Fine Wire Measurements at Vandenberg, AFB

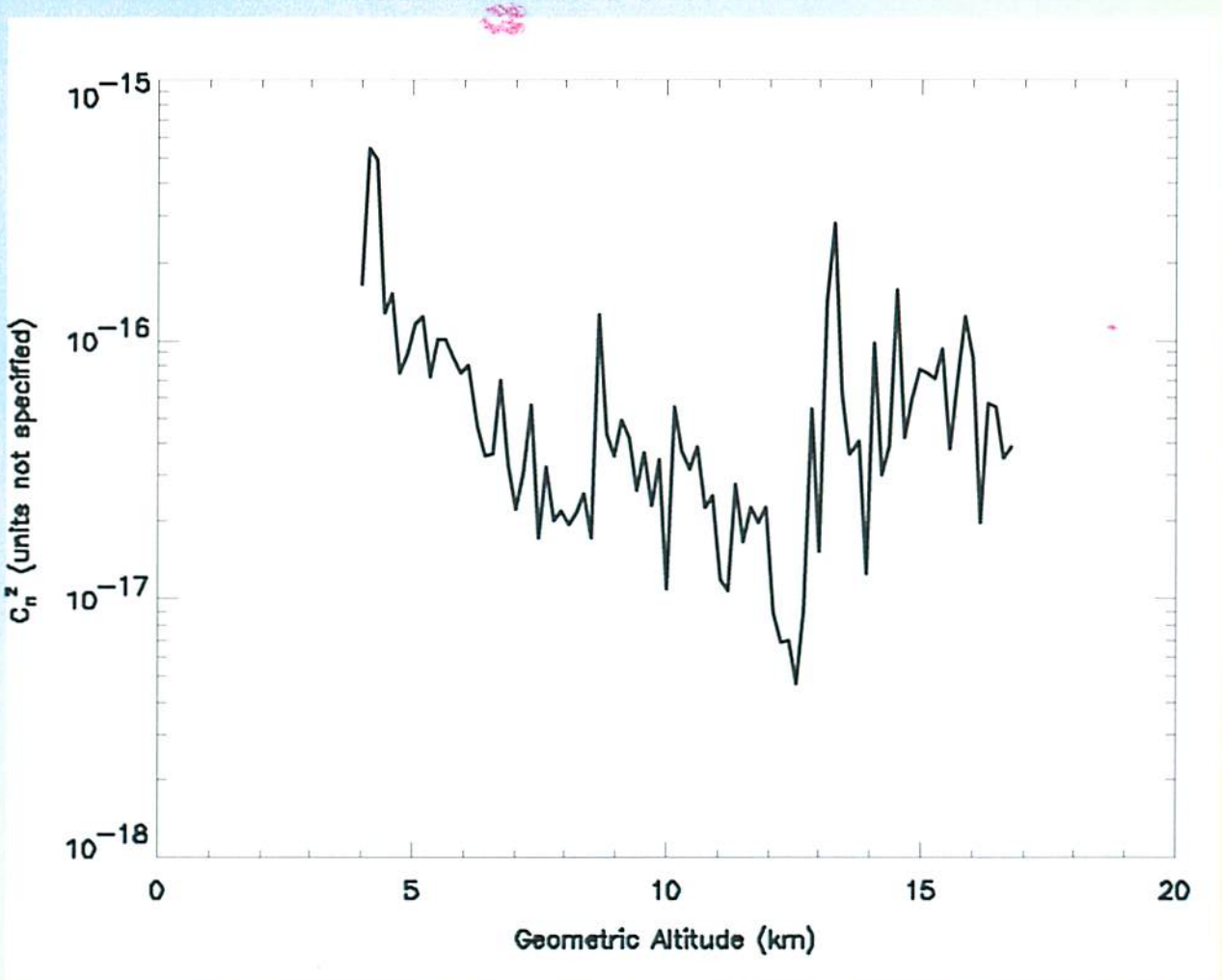

"Volume Filling" & ε vs. Cn2

$$\epsilon = \left(\gamma \bar{C}_n^2 \frac{N^2}{F^{1/3}} M^{-2} \right)^{3/2}$$

$$M = -77.6 \times 10^{-6} \frac{p}{T} \left(\frac{\partial \ln \theta}{\partial z} \right)$$

$$\times \left[1 + \frac{15{,}500q}{T} \left(1 - \frac{1}{2} \frac{\partial \ln q / \partial z}{\partial \ln \theta / \partial z} \right) \right]$$

Temperature Measurements in a Height Increment Equivalent to a Radar Range Gate

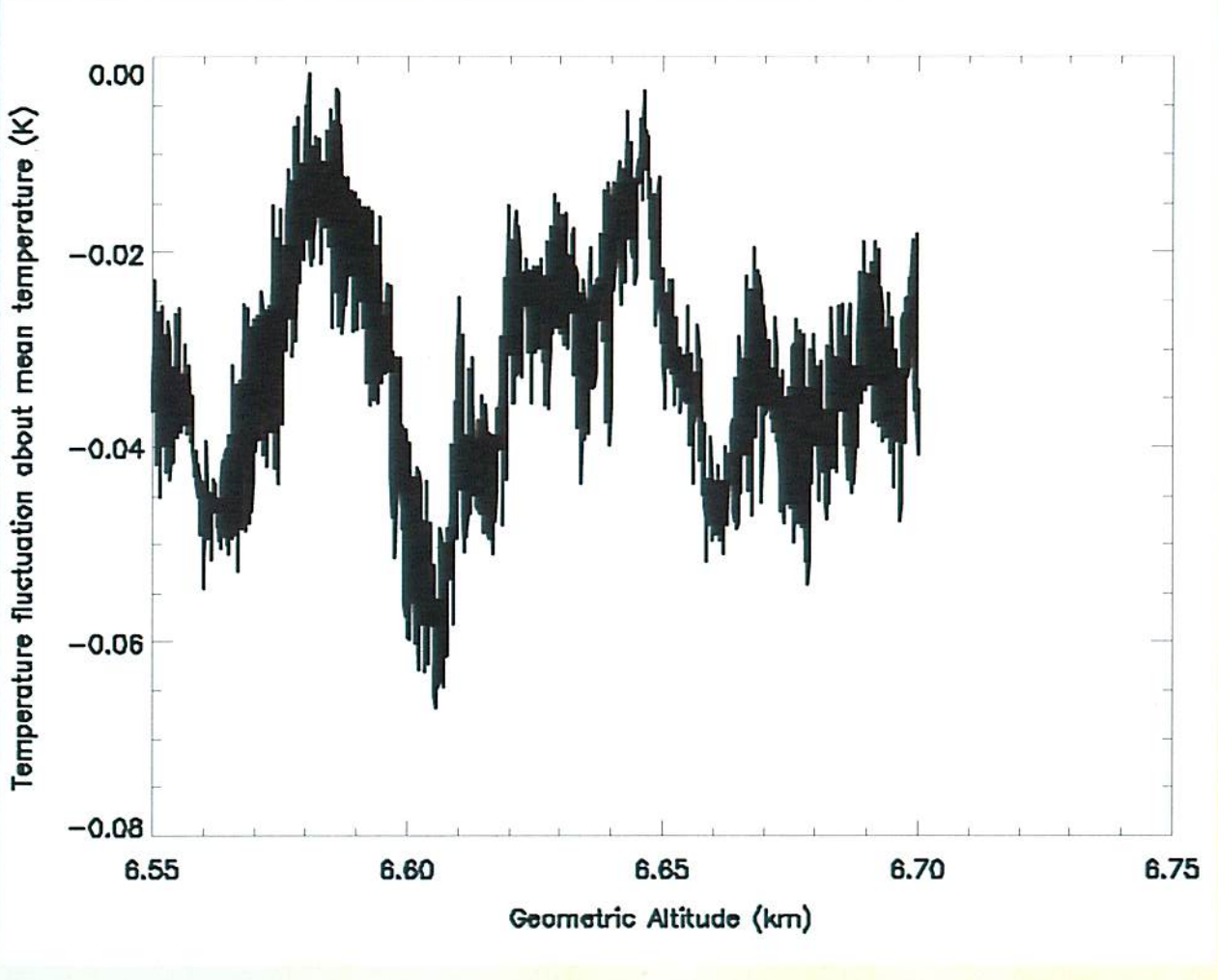

PSD of Fine Wire Temperature Measurements on June 14, 2007

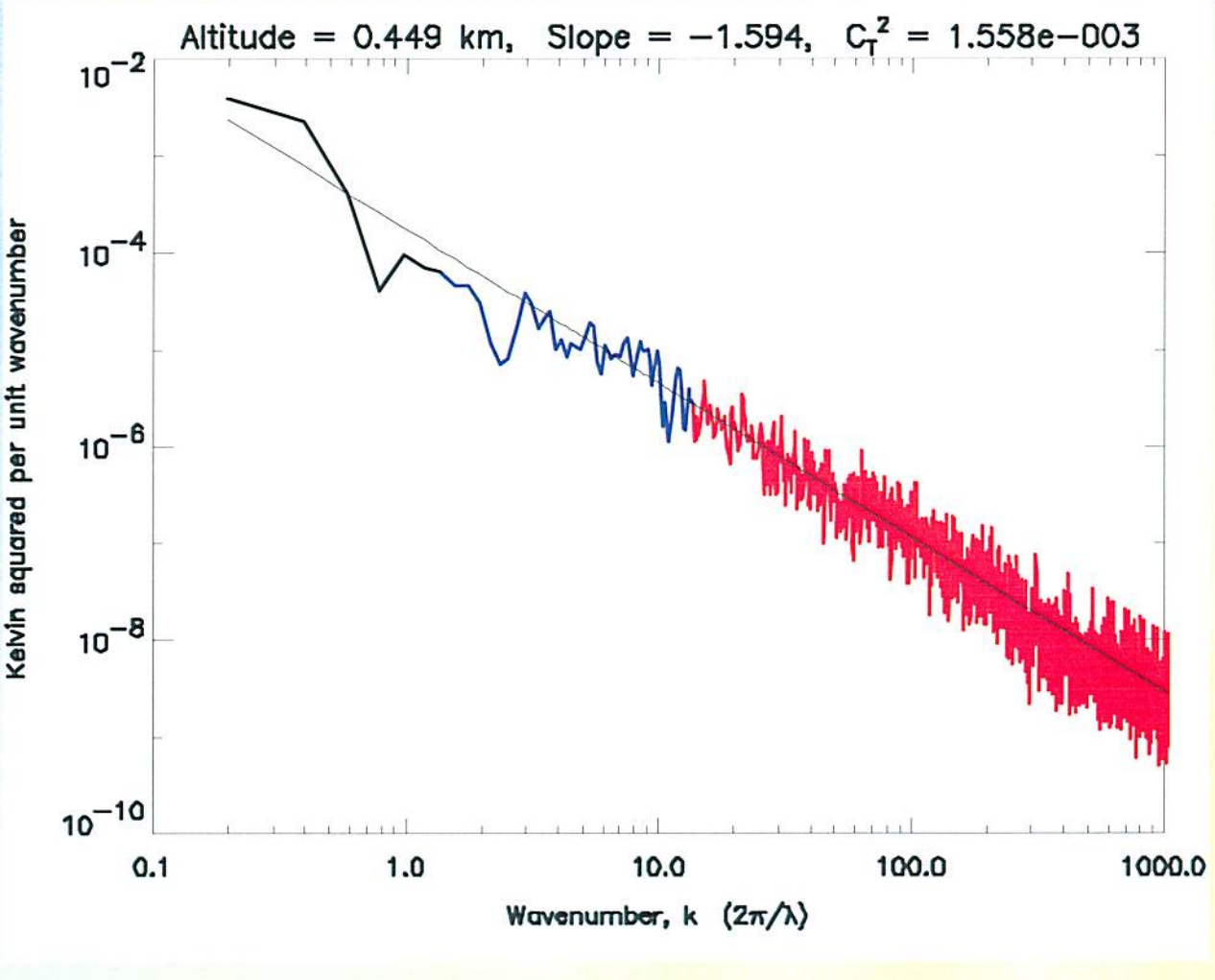

PSD of Fine Wire Temperature Measurements on June 14, 2007

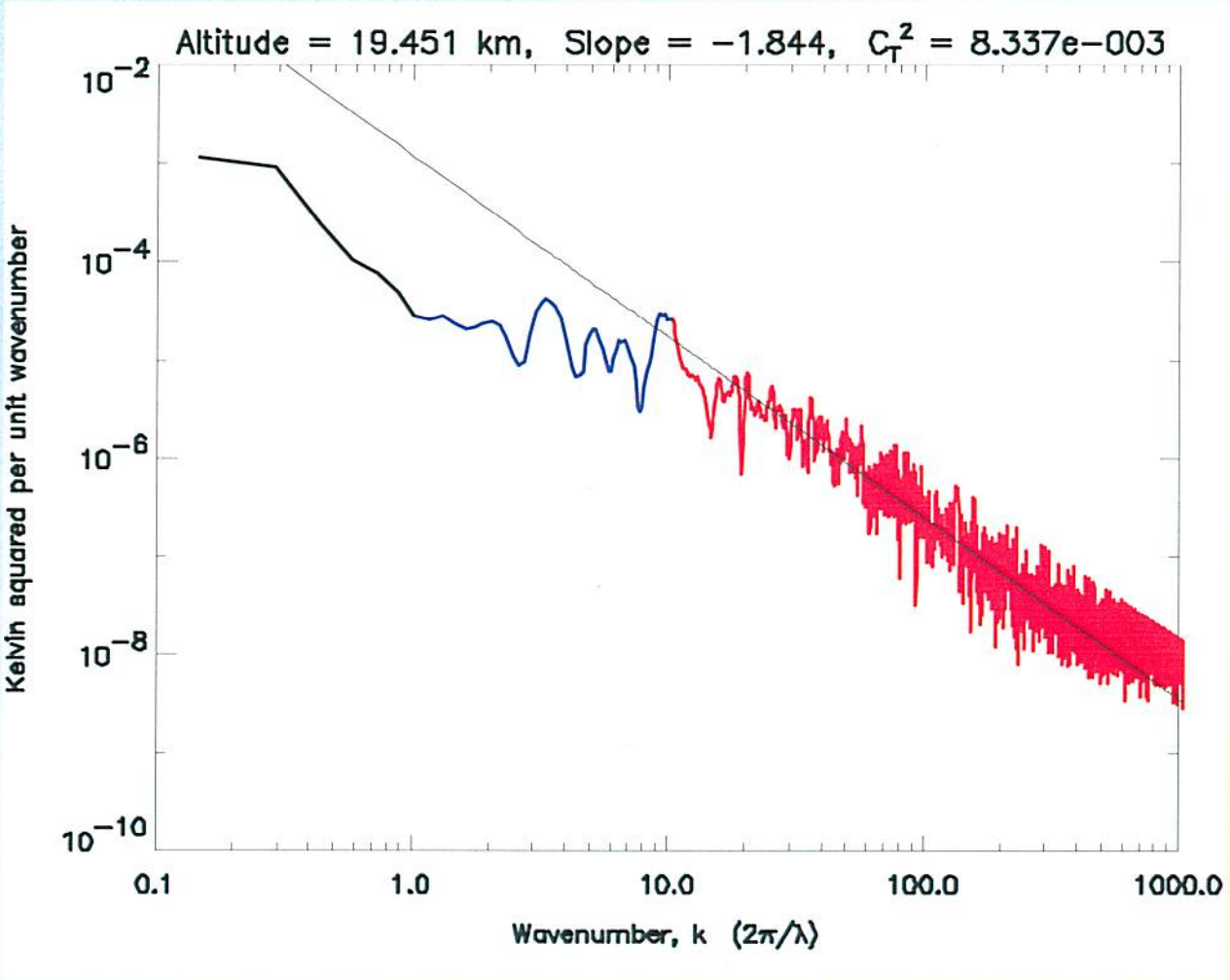

BEAM QUALITY AND IRRADIANCE ON TARGET

Mutual Coherence Function: $$\Gamma(\boldsymbol{\rho}, z) = \frac{w}{w_o} \exp\left[-s(\boldsymbol{\rho}, z) - \frac{\hat{z} k \boldsymbol{\rho}^2}{4z} - \frac{d(\boldsymbol{\rho}, z)}{2} \right]$$

where $$d(\boldsymbol{\rho}, z) = 8\pi^2 k^2 z \int_0^1 \int_0^\infty d\kappa \, d\xi \, \kappa \Phi_n(\kappa) \exp\left(\frac{-\hat{z} z \kappa^2 \xi^2}{k} \right) \left\{ 1 - J_o\left[(1 - \overline{\Theta} \xi) \kappa \rho \right] \right\}$$

$$s(\boldsymbol{\rho}, z) = 4\pi^2 k^2 z \int_0^1 \int_0^\infty d\kappa \, d\xi \, \kappa \Phi_n(\kappa) \left[1 - \exp\left(\frac{-\hat{z} z \kappa^2 \xi^2}{k} \right) \right]$$

Kolmogorov spectrum

$$\Phi_n(\kappa) = 0.033 \, C_n^2 \, \kappa^{-11/3}$$

Von Karman spectrum

$$\Phi_n(\kappa) = 0.033 \, C_n^2 \frac{\exp(-\kappa^2 / \kappa_m^2)}{(\kappa^2 + \kappa_o^2)^{11/6}}$$

Andrews spectrum

$$\Phi_n(\kappa) = 0.033 \, C_n^2 \frac{\exp(-\kappa^2 / \kappa_m^2)}{(\kappa^2 + \kappa_o^2)^{11/6}} \times \left[1 + 1.8(\kappa / \kappa_\ell) - 2.5(\kappa / \kappa_\ell)^{7/6} \right]$$

where $\kappa_m = 5.92 / \ell_o$ $\kappa_\ell = 3.3 / \ell_o$ $\kappa_o = 1 / L_o$

PSD Slopes

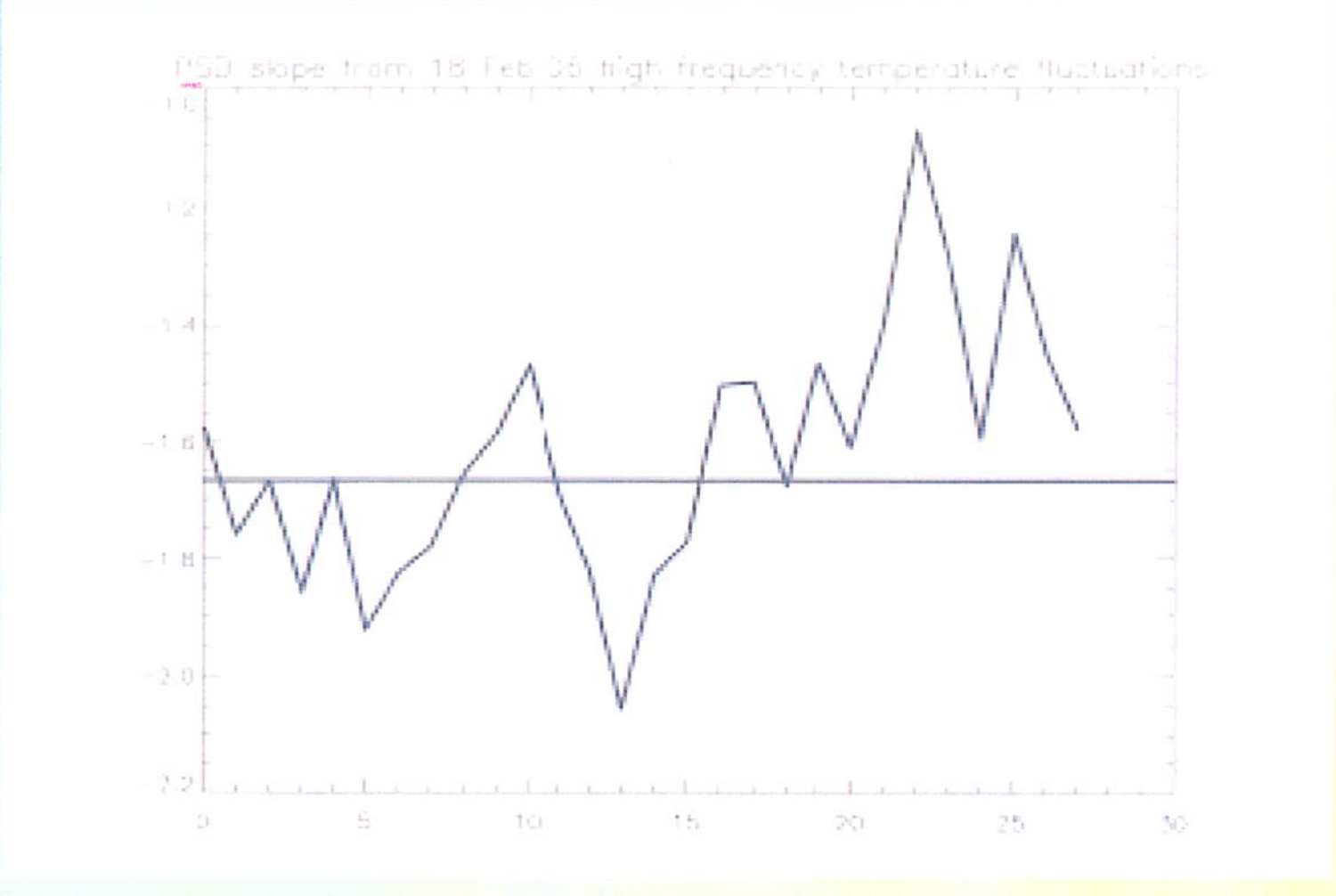
PSD slope from 18 Feb 00 high frequency temperature fluctuations
-1.0
-1.2
-1.4
-1.6
-1.8
-2.0
-2.2
0
5
10
15
20
25
30

Cn2 Without Dimensions

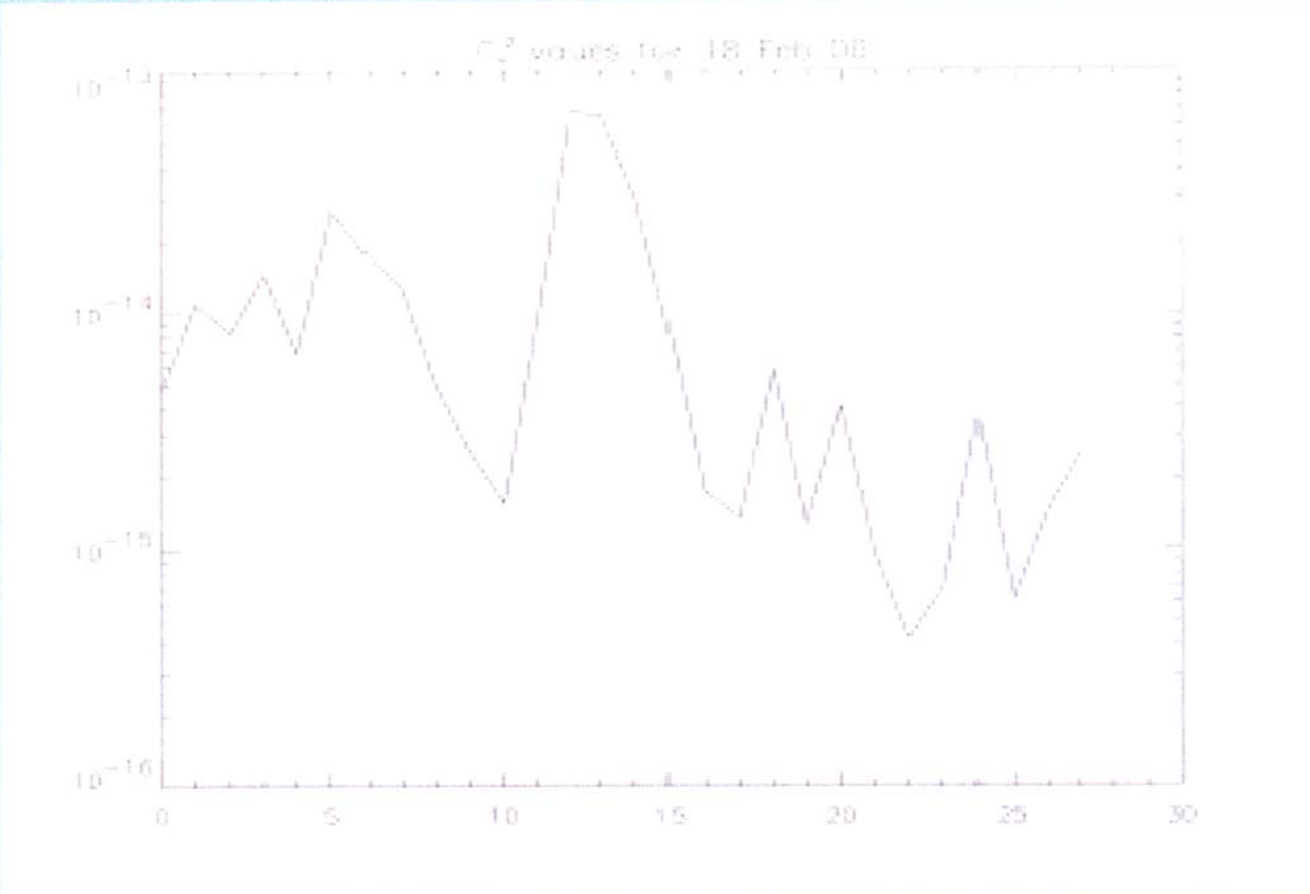

K-H and Low-level Waves

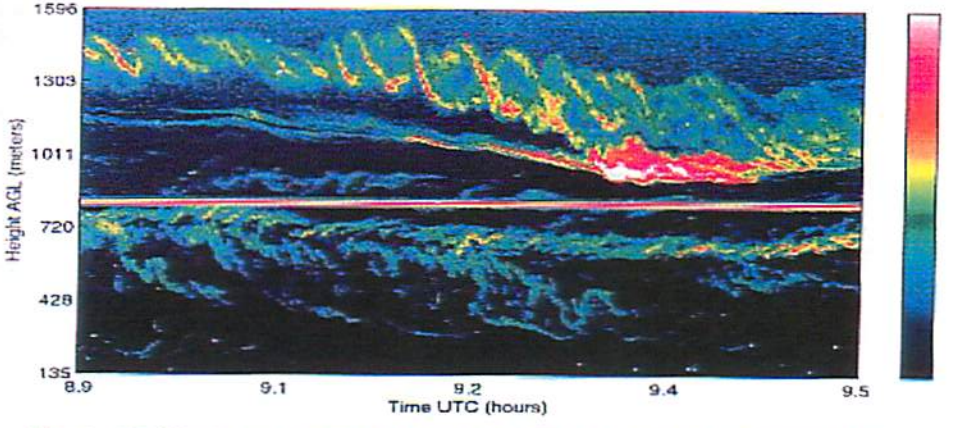

Plate 2. FMCW radar record showing the braided pattern of a Kelvin-Helmholtz instability on April 3, 1992. A color bar chart showing the order of colors used is included.

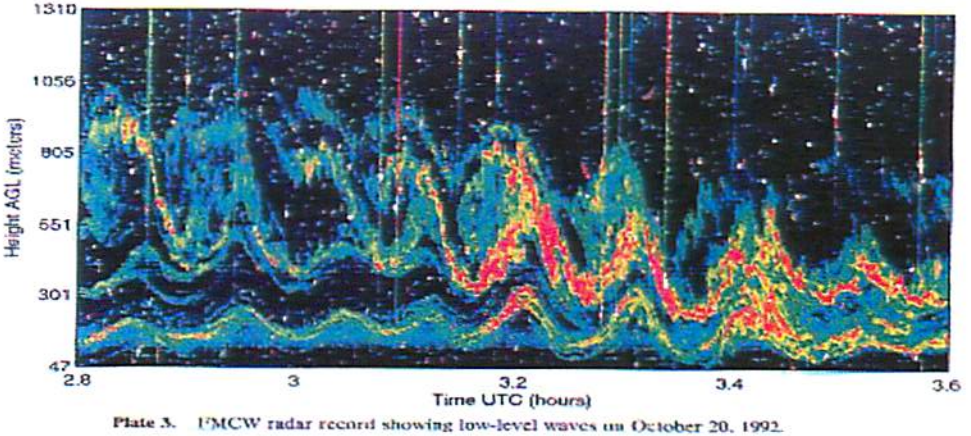

Plate 3. FMCW radar record showing low-level waves on October 20, 1992.

Convection and Winter Storm

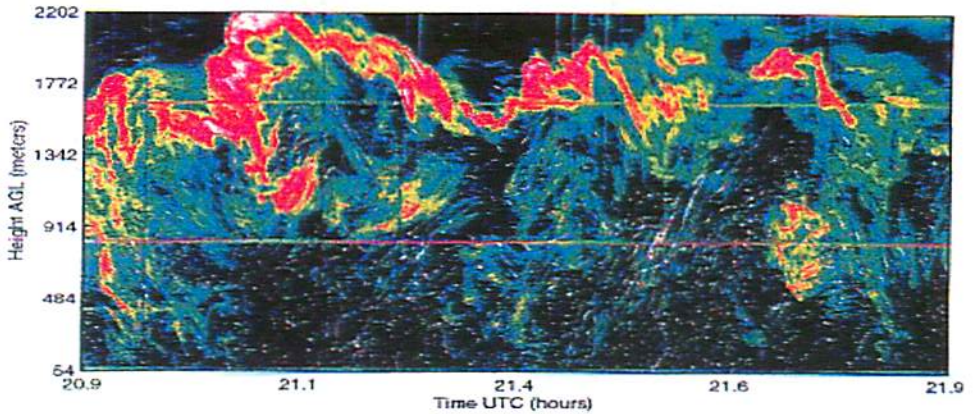

Plate 8. Midday boundary layer convection sensed by the FMCW radar on August 26, 1992. Insects act as tracers delineating the cell boundaries and providing flow visualization.

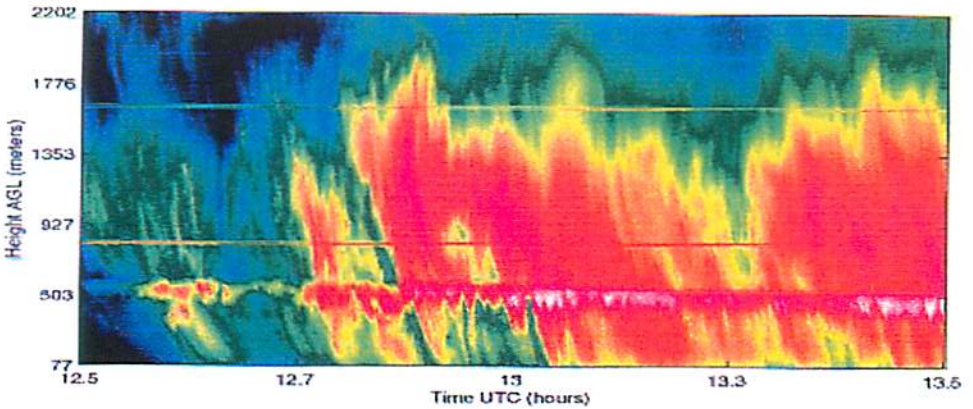

Plate 9. A light winter storm observed on January 21, 1992, with the FMCW radar. Changes in the "bright band" with time are clearly seen.

Summary

Methodology has been developed for additional experiments to address several issues related to optical turbulence. Measurement systems to be used include a balloon-ring platform system and a 50 MHz radar. Specific issues include: effects of path variability of Cn2 and inner scale on turbulent derived quantities over long paths, effects of "non-classical" turbulence on propagation including beam quality and irradiance on target, the "volume filling" radar problem, relationship between mechanical and optical turbulence, and improved understanding of radar scattering mechanisms.

DISTRIBUTION LIST

DTIC/OCP
8725 John J. Kingman Rd, Suite 0944
Ft Belvoir, VA 22060-6218 1 cy

AFRL/RVIL
Kirtland AFB, NM 87117-5776 2 cy

Frank Eaton
Official Record Copy
AFRL/RDSEW 1 cy